Galactic Cosmic Ray Variation Caused by Different Structural Elements of Isolated Earth-Impacting Coronal Mass Ejection

Darije Maričić[1], Filip Šterc[1], Antony Belov[2], Dragan Roša[1], Damir Hržina[1] and Ivan Romštajn[1]

[1]*Astronomical Observatory Zagreb, Opatička 22, HR-10000 Zagreb, Croatia*
(email: dmaricic@zvjezdarnica.hr, drosa@zvjezdarnica.hr, fsterc@zvjezdarnica.hr, dhrzina@zvjezdarnica.hr, iromstajn@zvjezdarnica.hr)
[2]*IZMIRAN, Russian Academy of Science, Moscow, Russia*
(email: abelov@izmiran.ru)

The fifth Meeting on Astrophysical Spectroscopy - A&M data
Astronomy & Earth Observation
12 - 15 September 2023, Palić, Serbia

Introduction

– List of isolated Earth-impacting interplanetary coronal mass ejection (ICMEs) that cover the period from January 2008 to August 2014, published in Maričić+ (2020) serve as a starting point for this analysis. (the period during which the data from both STEREO satellites are available) and list of the solar wind disturbances (SWD).

– We separated ICMEs on: I) single and interacting

– Made additional analysis regarding to low-corona signatures (LCS)
(connection with flares, prominences and ARs)

– Again, we separated ICMEs on II) direct and flank encounter

– Accompanied ICMEs kinematics with coresponding solar wind disturbances (SWD) and variation of CR density, A_0.

– We divided the isolated Earth-impacting ICME structure to three different structural elements defined as: the turbulent sheath (TS), the frontal region (FR), and the magnetic obstacle (MO) itself.

– Established correlation between the parameters of the solar wind disturbances and the variation of CR density for those three different segments of the ICME.

– We investigate the characteristics of short-term reductions in galactic cosmic ray (GCR) flux (Forbush decreases, FD), within different structural elements of isolated Earth-impacting ICMEs.

The data set

– For the period from January 2008 to August 2014 - 282 solar wind disturbances were recognized - SWD for the analysis at L1 point we used the WIND Magnetic Field Investigation (MFI) and Solar Wind Experiment (SWE) data, 1 minute resolution, GSE coordinates, accompained with ACE data.
http://wind.nasa.gov/mfi_swe_plot.php / http://www.srl.caltech.edu/ACE/ASC/level2/index.html

– For recognizing of the accompanied ICME we used data from **STEREO** satellites - **SECCHI-COR2** Outer Coronagraph and **SECCHI-HI** Heliospheric Imager http://stereo-ssc.nascom.nasa.gov/browse/ and **SOHO** satellite - **LASCO C2 / C3** Coronagraphs http://lasco-www.nrl.navy.mil/daily_mpg/

– For additional information of LCS, we used the

SDO/EVE SAM pinhole camera - http://lasp.colorado.edu/eve/data_access/

SDO Atmospheric Imaging Assembly (AIA) and Helioseismic Magnetic Imager (HMI) http://sdo.gsfc.nasa.gov/data/

– Futhermore, we used the database of variation of cosmic rays (VCR) / Forbush effect created by Pushkov Institute of terrestrial magnetism, ionosphere and radio wave propagation, (IZMIRAN Cosmic Ray Group).

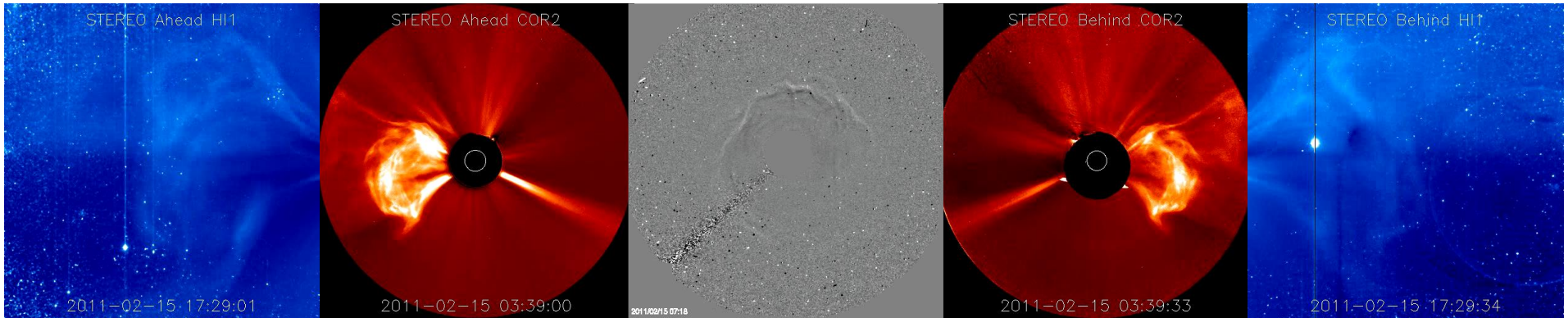

ICME direction

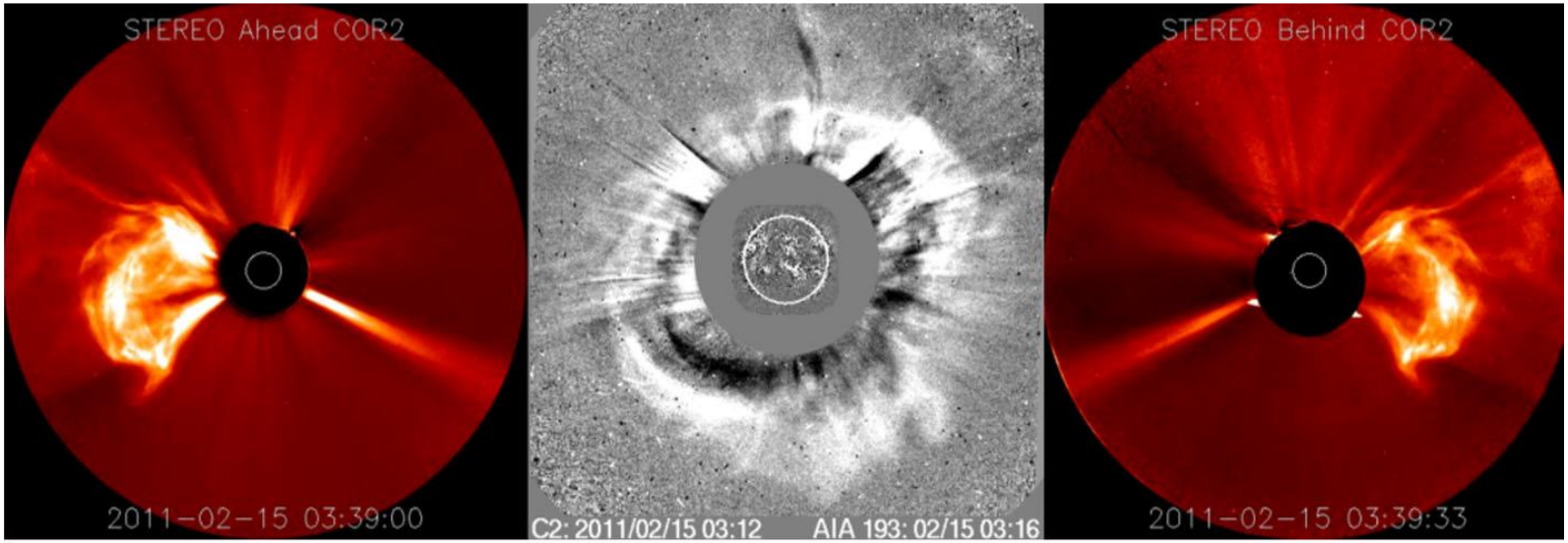

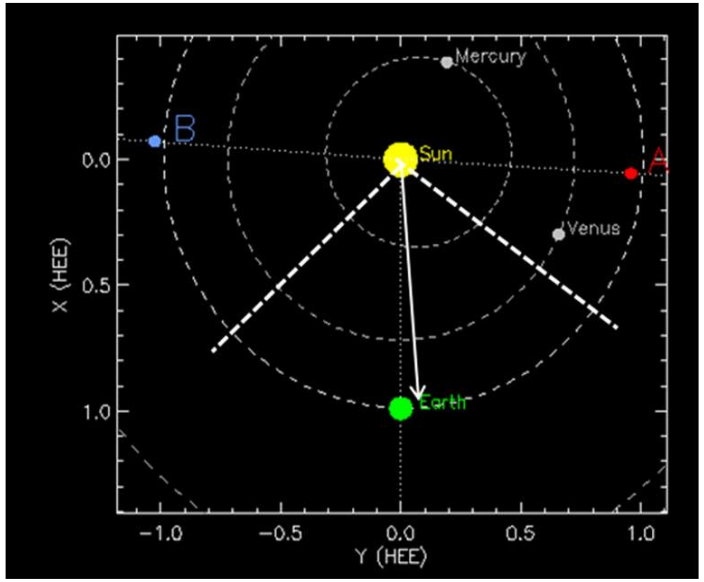

Top: Snapshots of the CME of 15 February 2011 provided by STEREO-A COR2 (left), SOHO LASCO C2 (middle) with inserted AIA 19.3 nm filtergram (running difference images are presented), and STEREO-B COR2 (right). We selected the time period from January 2008 to August 2014.

Bottom: spacecraft positions and the CME propagation direction (white arrow).
The two dashed lines depict the cone within which the CME is expected to propagate.

In this way, we found that out of the identified 1644 CMEs, 439 (≈ 27%) were potential candidates for Earth-impacting ICMEs. A list of CMEs observed by all three spacecraft, containing basic information on all 1644 events, is published online at https://zvjezdarnica.hr/pdf/ListICMEs.pdf.

ICME kinematic

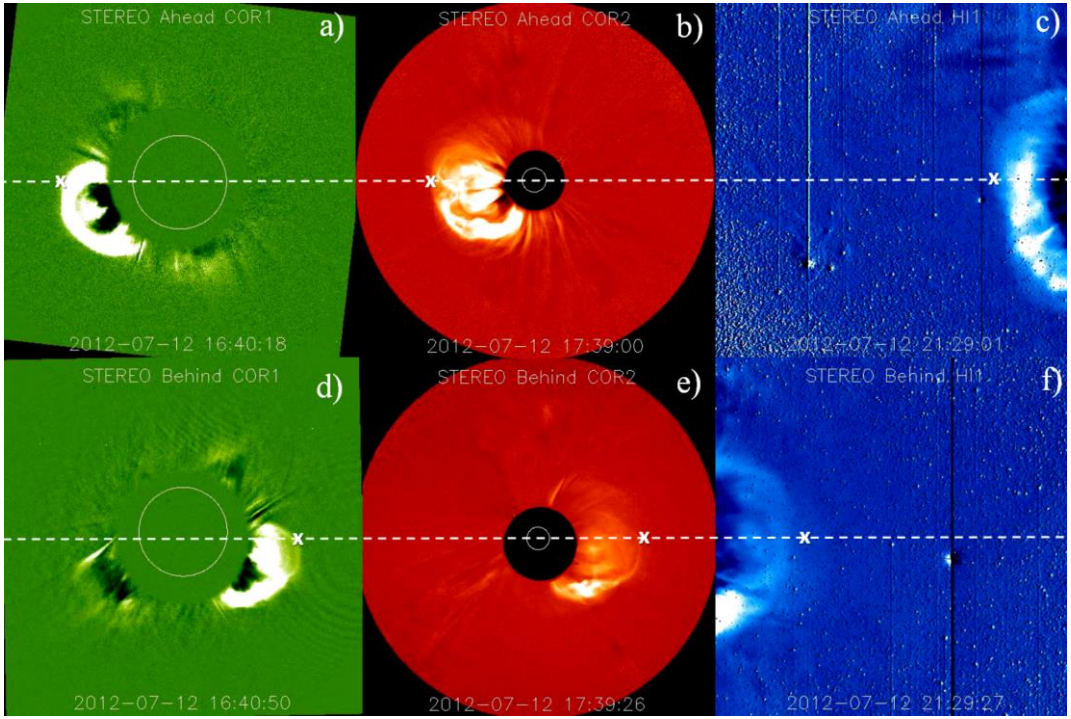

Number of ICMEs when comparing COR2 ICME detections and *WIND* solar wind disturbances for the period January 2008 to August 2014

List	Number of CMEs
CME list	1644
SWD list	282
Non Earth-directed CMEs	1205
Earth-directed ICMEs, i.e. candidates Earth-direstes CMEs for	439
Confirmed Earth-impacting ICMEs with 67 *in situ* SW signatures	103
Single Earth-impacting ICMEs	31
Single Earth-impacting ICMEs with MO	17

Note. Our method generated a list of 439 candidates for Earth-directed ICMEs, which was reduced to 103 confirmed Earth-impacting ICMEs.

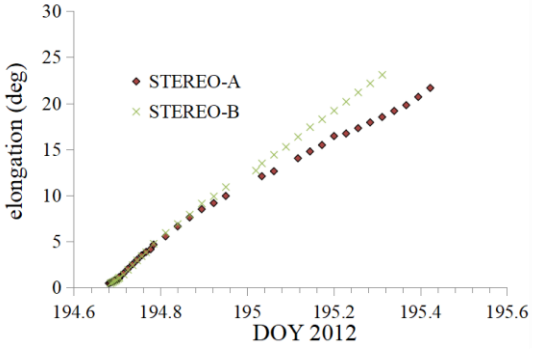

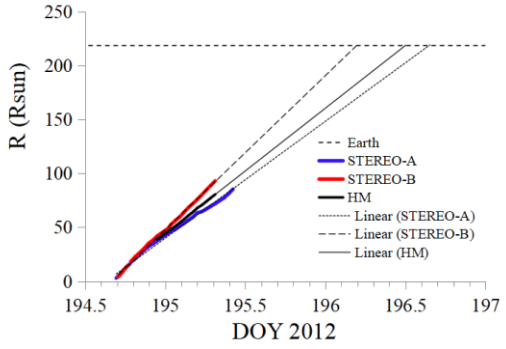

- from elogation-time, using HM approximation, we calculate direction and arrival time of ICME at Earth distance. method published in Maričić+ (2020)

Solar wind disturbances – online catalog

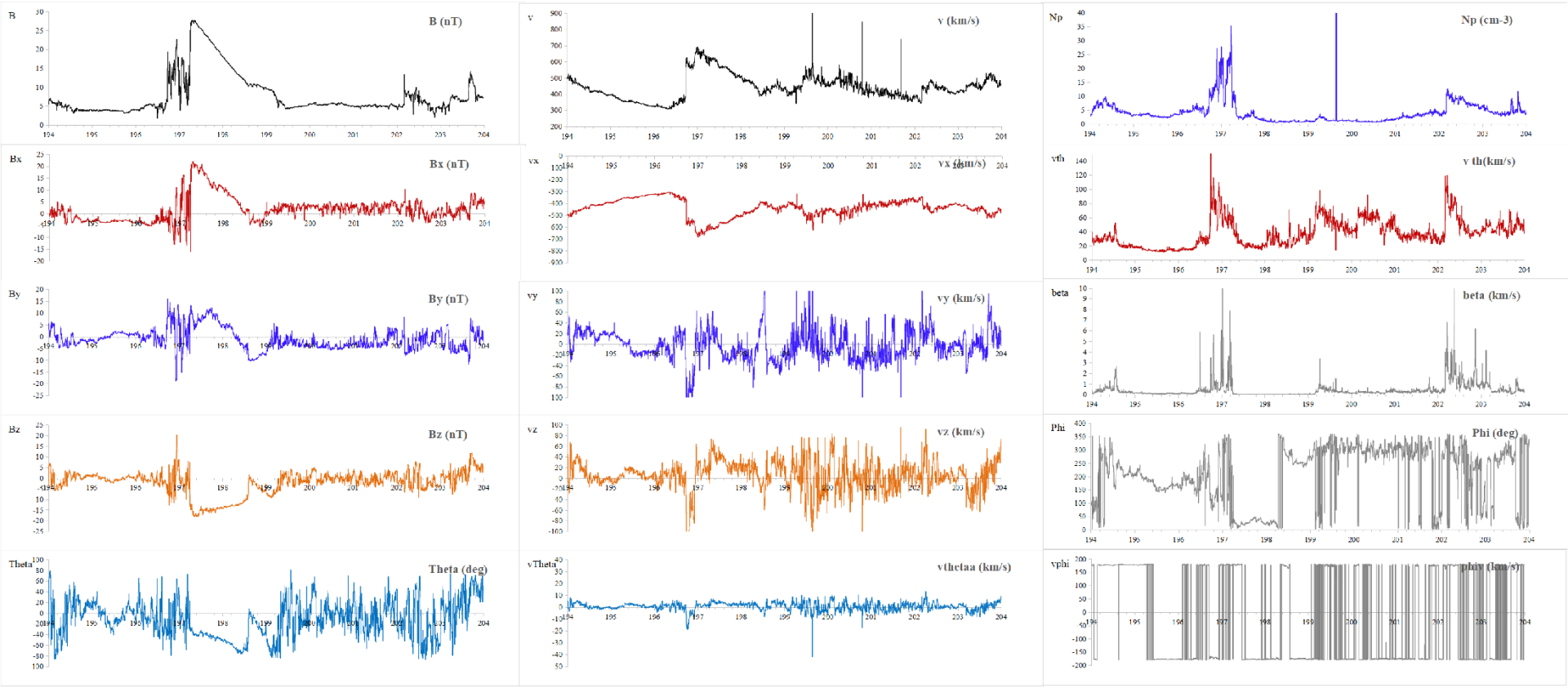

- for period from **January 2008 to August 2014** - recognized 282 solar wind disturbances – online catalog for general use: https://zvjezdarnica.hr/pdf/ListSWDs.pdf
- the SW events where identified by detailed inspection of the plasma and magnetic field structure Dumbović+ (2012), Kilpua+ (2013), Paouris+ (2017) and the references therein
- for 103 out of 439 ICME-s it was possible to connect with 67 corresponding solar wind disturbances

ICMEs morphology

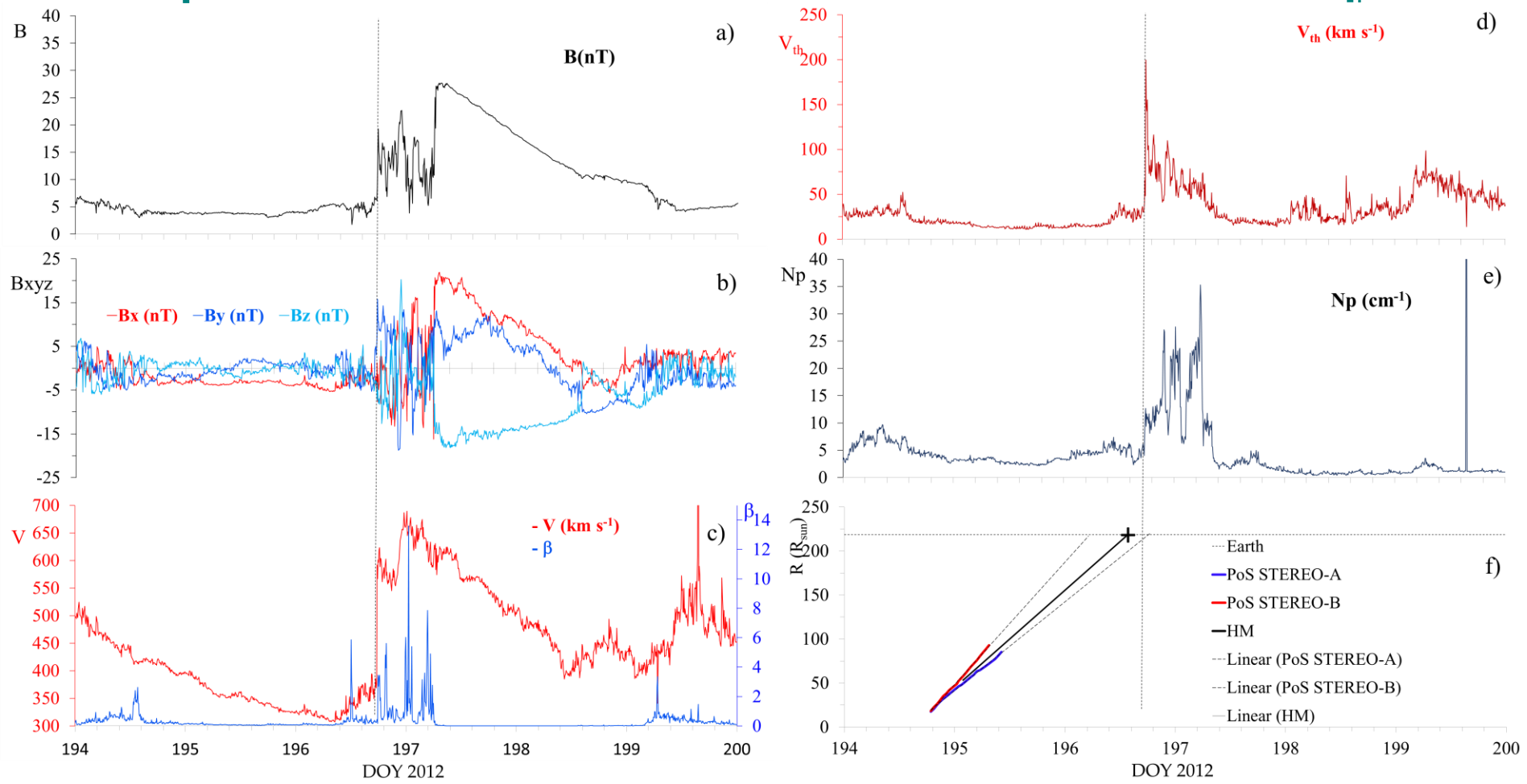

the period (DOY = 194 - 200) from 12 to 18 July 2012

Example of an isolated Earth-impacting MO-ICME on 12 July 2012.

(a) magnetic field magnitude, (b) GSE magnetic field components, (c) solar wind speed and plasma-beta (plasma-to-magnetic pressure ratio), (d) thermal velocity, (e) proton density, and (f) overall kinematics of the ICME.

.

ICMEs *interaction*

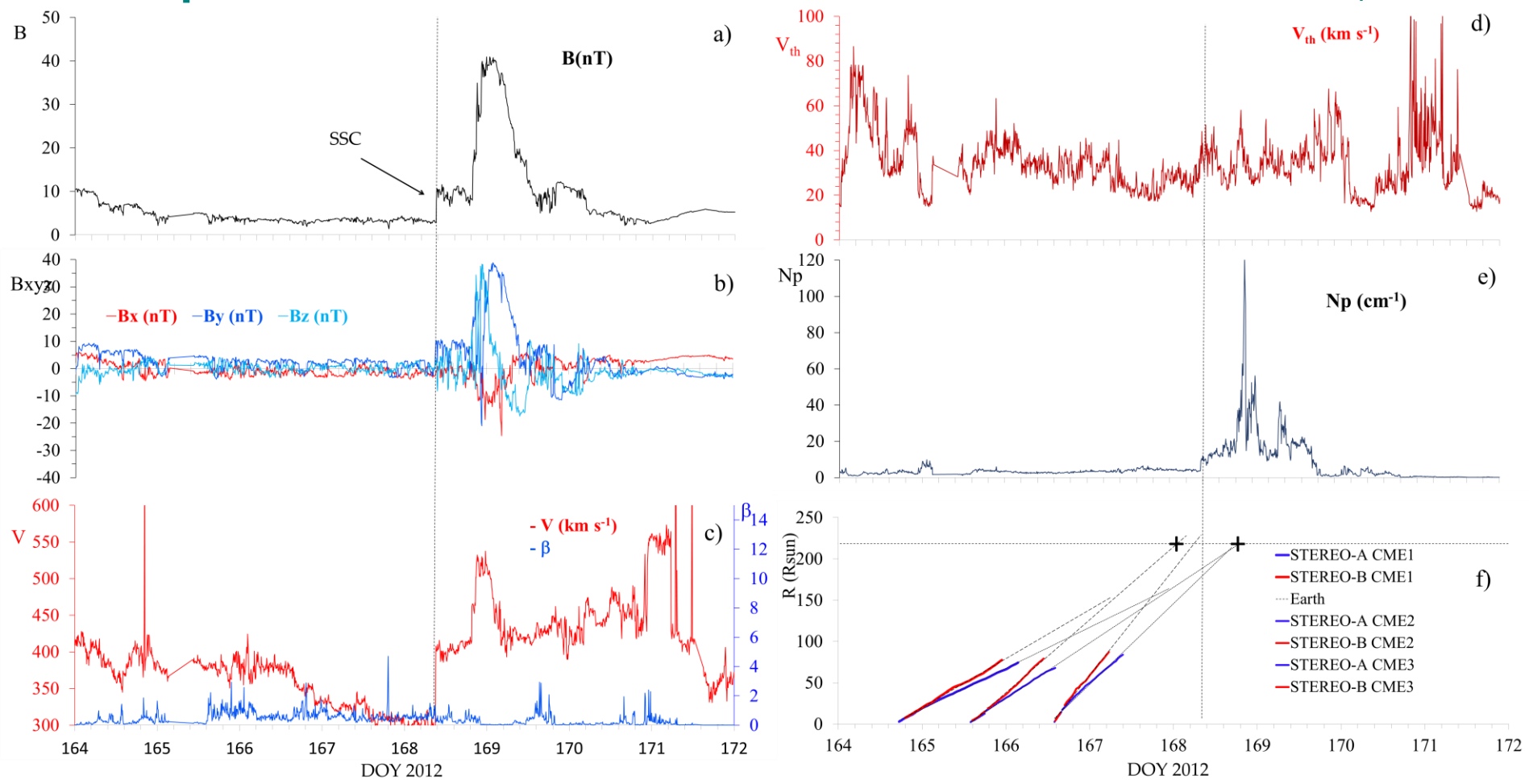

the period (DOY = 164 - 172) from 12 to 20 June 2012

- *e*xample of an ICME interaction event. The CMEs that erupted on 12, 13, and 14 June 2012 (DOY = 164 – 166), respectively
- 103 ICMEs we associated with 67 SWD.
- *31 of them caused by single arriving ICME* (~46% of all analysed SW disturbances), *34 by CME-CME interaction* (~51% of all SW disturbances) and *2 by CME – CIR/HHS interaction* (~3% of all analysed SW disturbances).

MO- or EJ- ICMEs

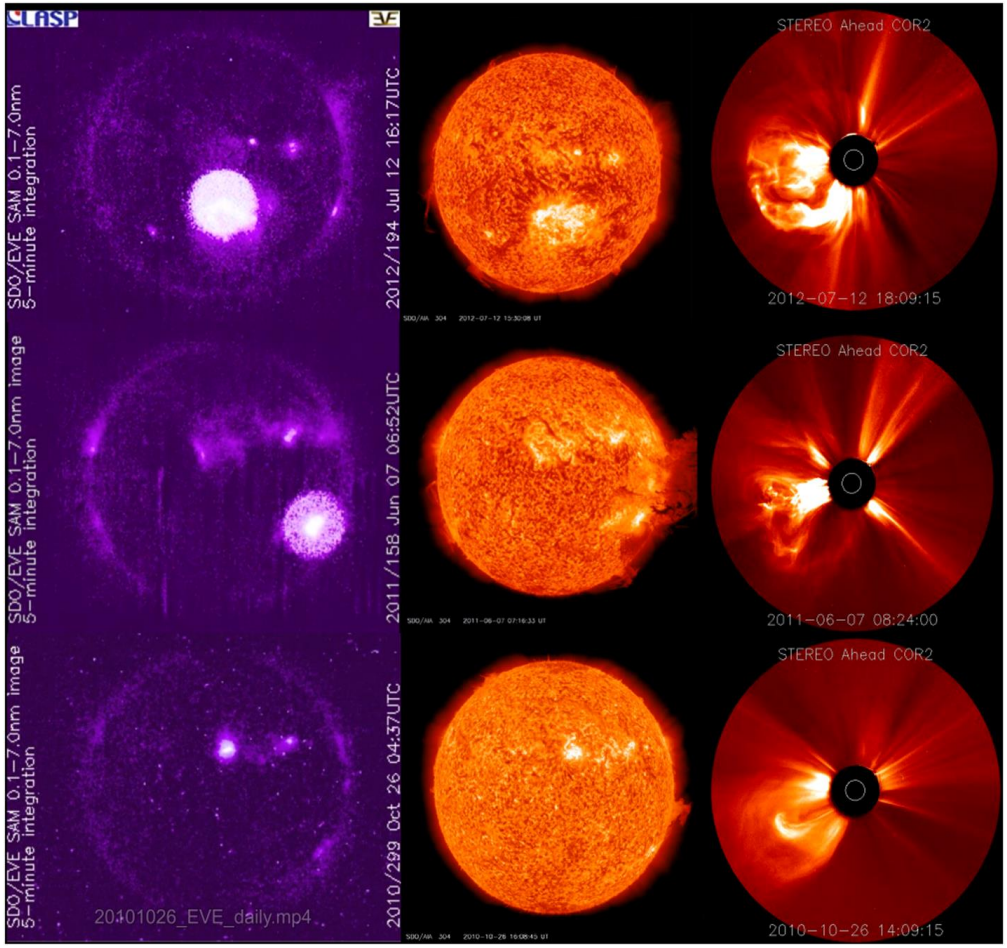

Three examples of isolated Earth-impacting ICMEs (from top to bottom: 12 July 2012, 7 June 2011, and 26 October 2010), recorded by the SDO/EVE SAM pinhole camera, the SDO/AIA 304 Å filter, and the COR2 STEREO-A coronagraphs (from left to right).

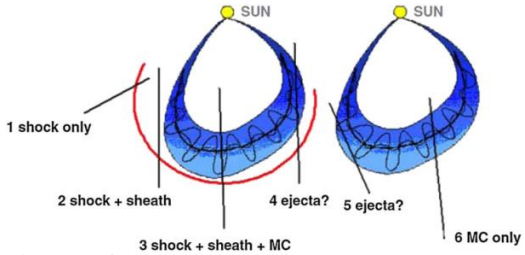

image form Kim et al. (2008)

EJ-ICMEs with a source location longitude larger than ±30◦ from the central meridian, cause a specific signature in the solar wind in situ data

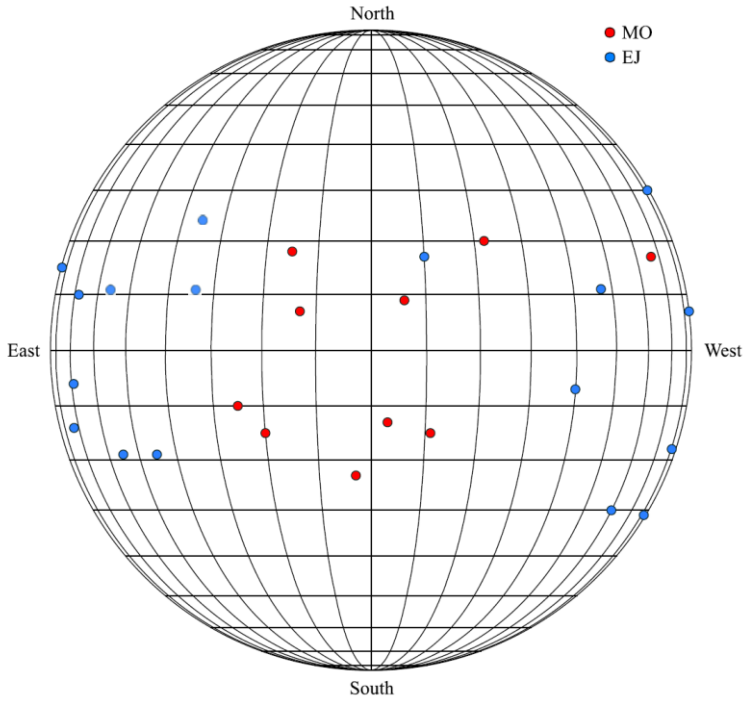

MO- vs EJ- ICMEs – direct or flank

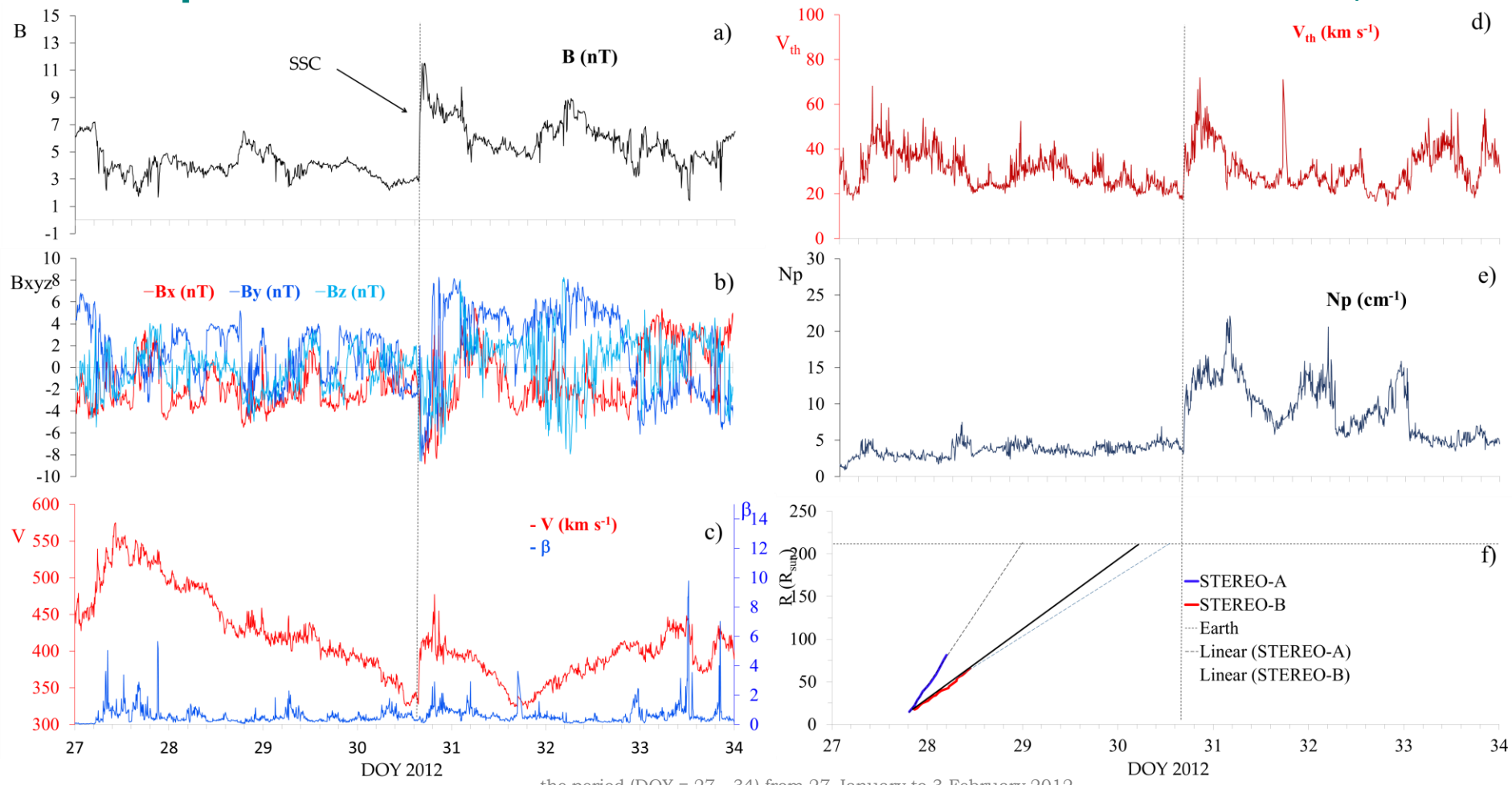

the period (DOY = 27 - 34) from 27 January to 3 February 2012

Example of an EJ-ICME showing in situ Wind signatures at L1 (DOY = 27 is 27 January 2012).

EJ-ICMEs with a source location longitude larger than 30◦ from the central meridian, cause a specific signature in the solar wind in situ data.

In this way, 17 MO-ICMEs and 14 EJ-ICMEs were identified.

ICMEs morphology

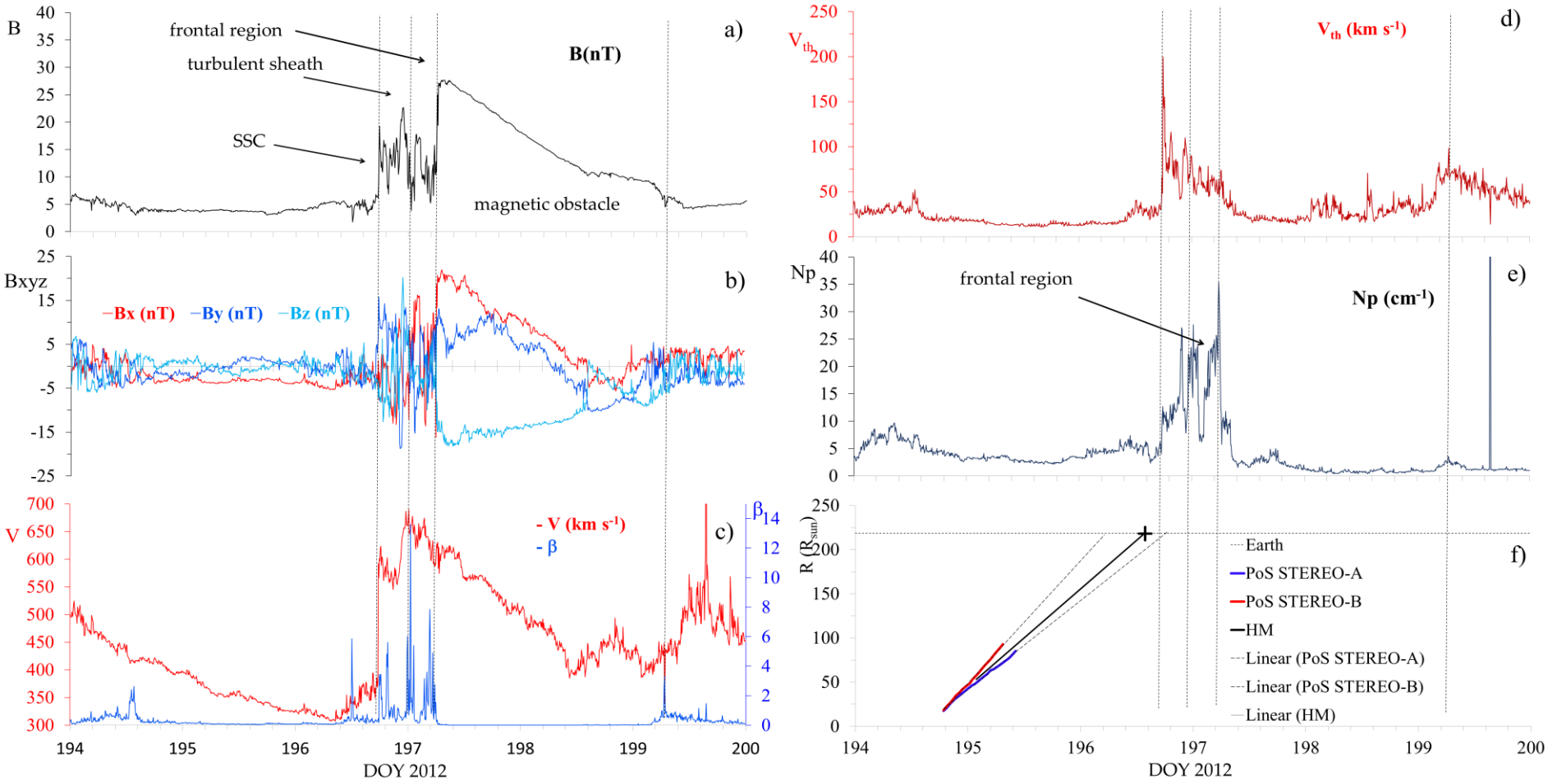

the period (DOY = 194 - 200) from 12 to 18 July 2012

For identifying the ICME structural elements - we used a series of criteria: (e.g., Kim+ 2013), (Belov+ 2014). First we consult: the plasma-β parameter, an increased intensity of the interplanetary magnetic field (IMF) variations; An abnormally low proton temperature (T); A decrease of the solar wind velocity; A decrease of the plasma density;

ICMEs morphology

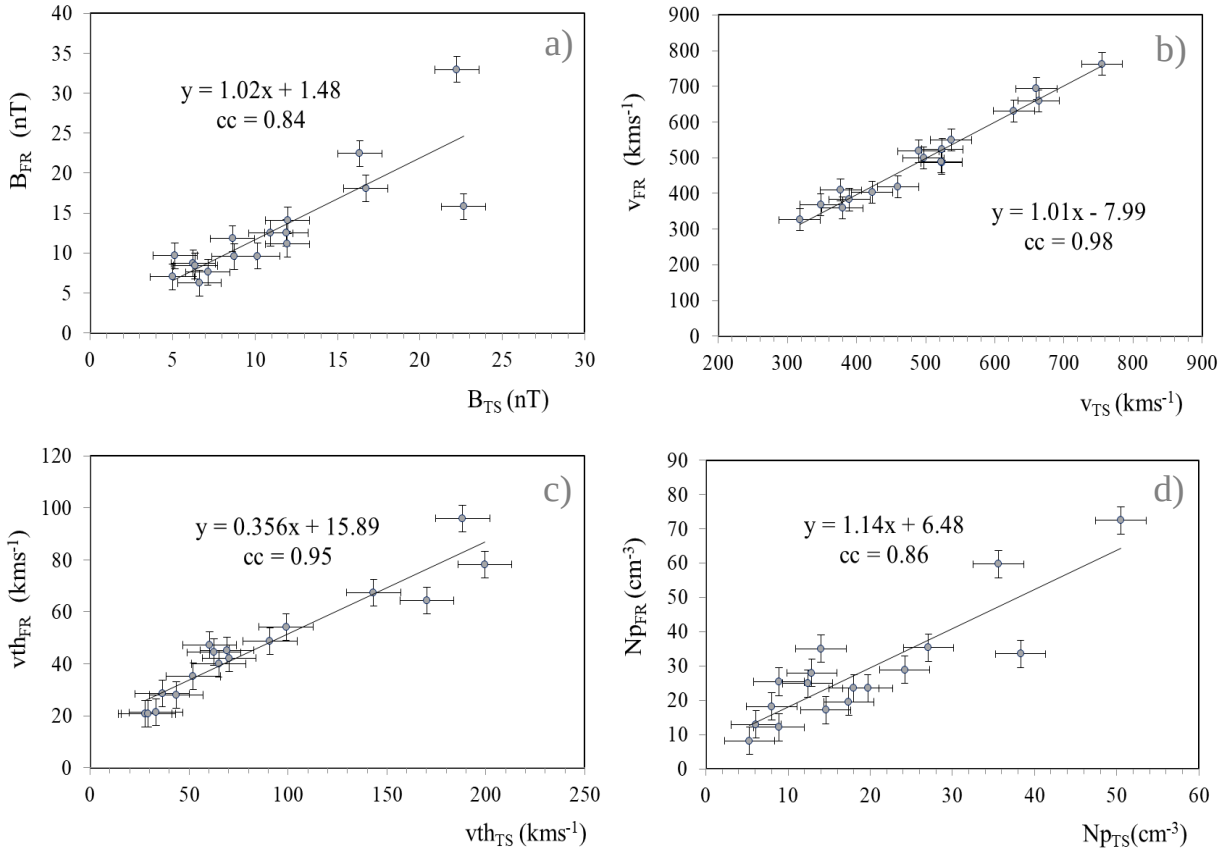

from (Maričić+ 2020)

The TS/FR correlations, of the four basic solar wind parameters (magnetic field strength, B_{max}, flow speed, v_{max}, proton thermal speed, vth_{max}, and proton density, Np_{max}).

ICMEs – frontal region vs turbulent sheat

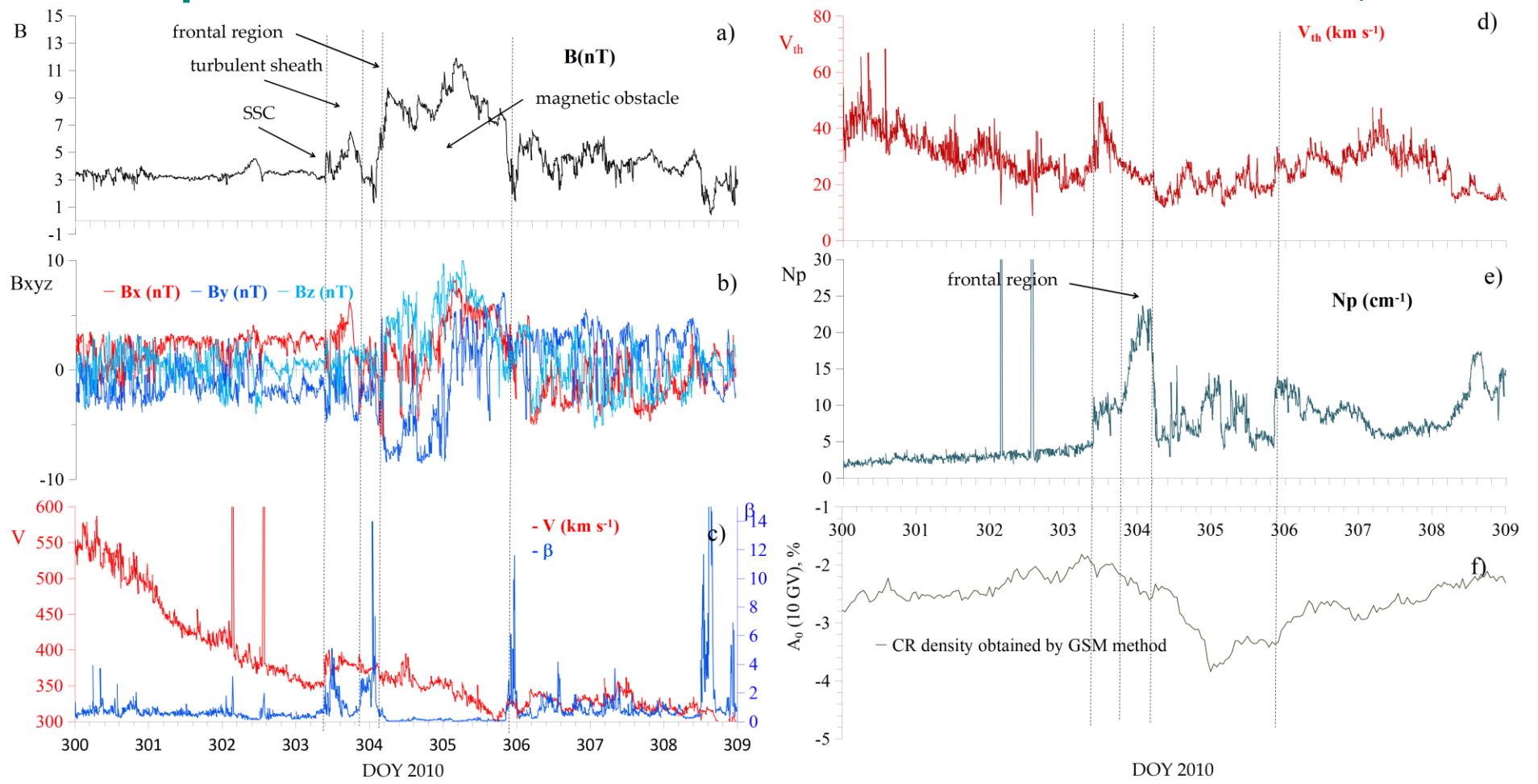

the period (DOY = 300 - 309) from 27 October to 5 November 2010

(a) magnetic field magnitude, (b) GSE magnetic field components, (c) solar wind speed and plasma-beta (plasma-to-magnetic pressure ratio), (d) thermal velocity, (e) proton density, and (f) density of the CR a rigidity of 10 GV. FR is a part of the ICME characterized by an additional enhancement of proton density and decrease of the flow speed can be often recognized.

MO - ICMEs

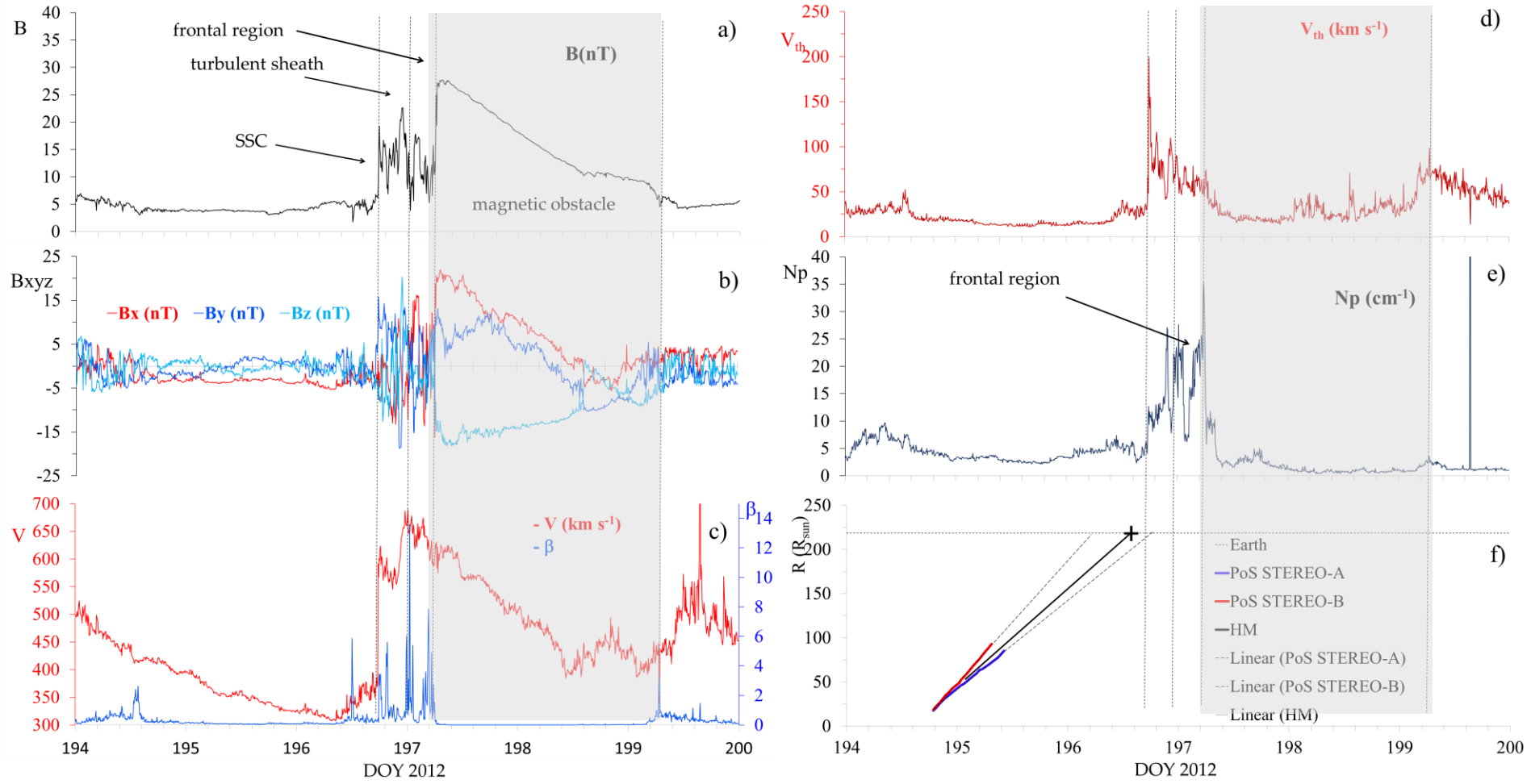

the period (DOY = 194 - 200) from 12 to 18 July 2012

We adopt the terminology used by Jian et al. (2006) and Nieves-Chinchilla et al. (2018), where an ICME is denoted as a "magnetic obstacle" (MO) even if a small region with typical MC signatures is identified, i.e. when the ICME configuration is not associated with a full single magnetic field rotation.

ICMEs - SW parameters vs CR variation

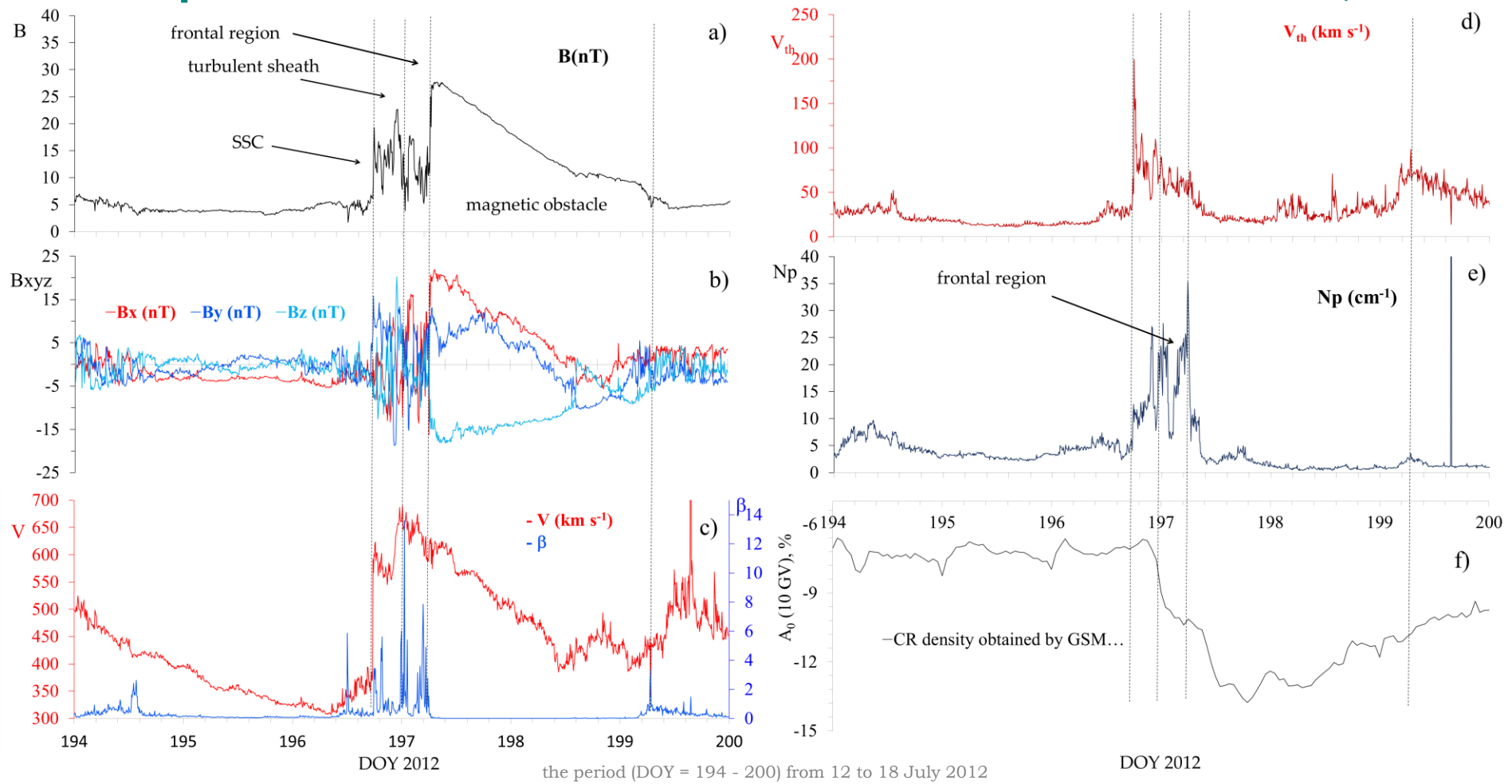

the period (DOY = 194 - 200) from 12 to 18 July 2012

I) Example of an isolated Earth-impacting where **MO and TS + FR caused roughly equal variation of CR density** / (9/17, 53%) **two-step profile**

(a) magnetic field magnitude, (b) GSE magnetic field components, (c) solar wind speed and plasma-betapharameter, (d) thermal velocity, (e) proton density, and (f) the variation of CR density at a fixed rigidity of 10 GV.

ICMEs - SW parameters vs CR variation

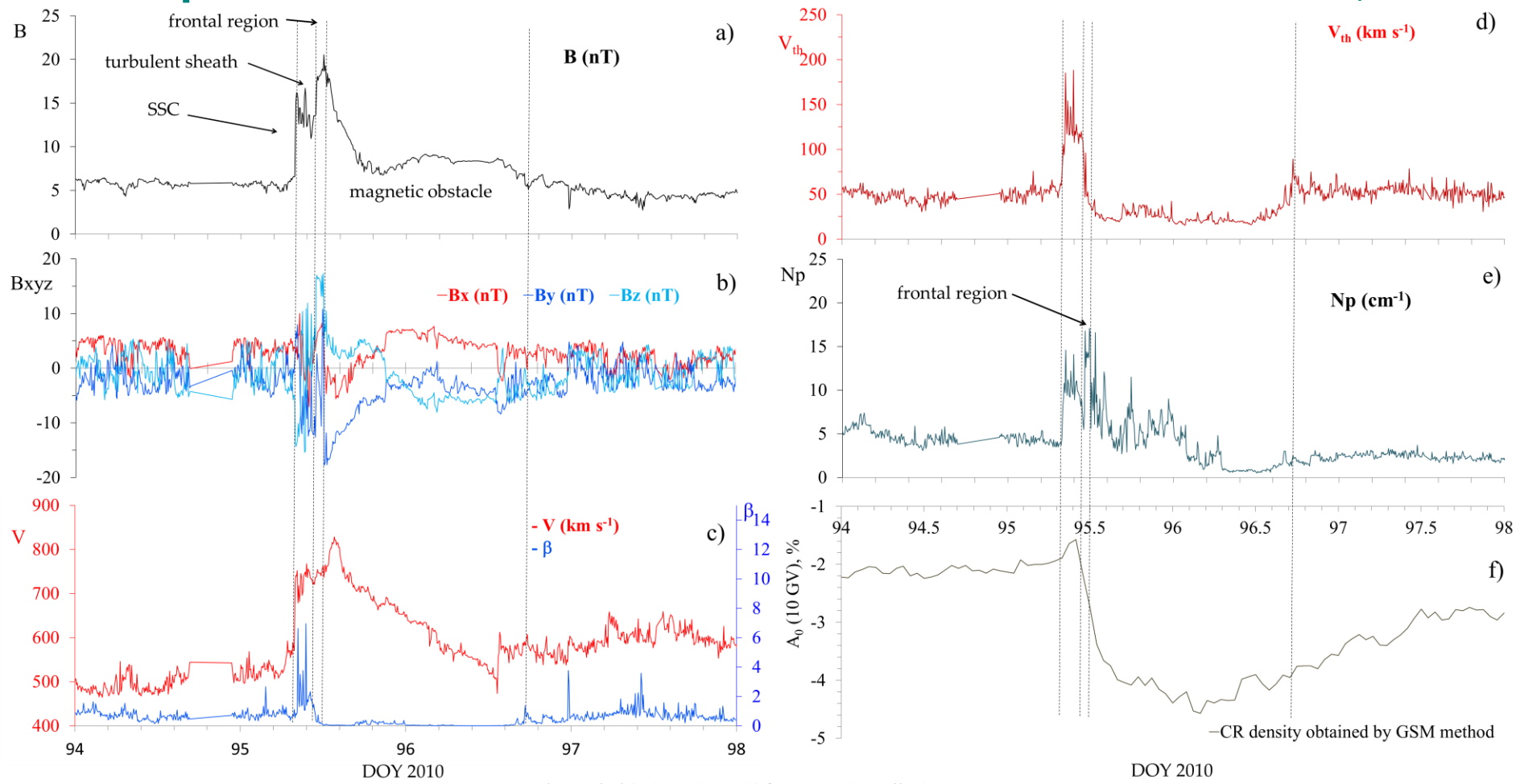

the period (DOY = 94 - 98) from 4 to 8 April 2010

Example of an isolated Earth-impacting where **MO and TS + FR have caused roughly equal variation of CR density**. (7/17, 41%) / **one-step profile**

ICMEs - SW parameters vs CR variation

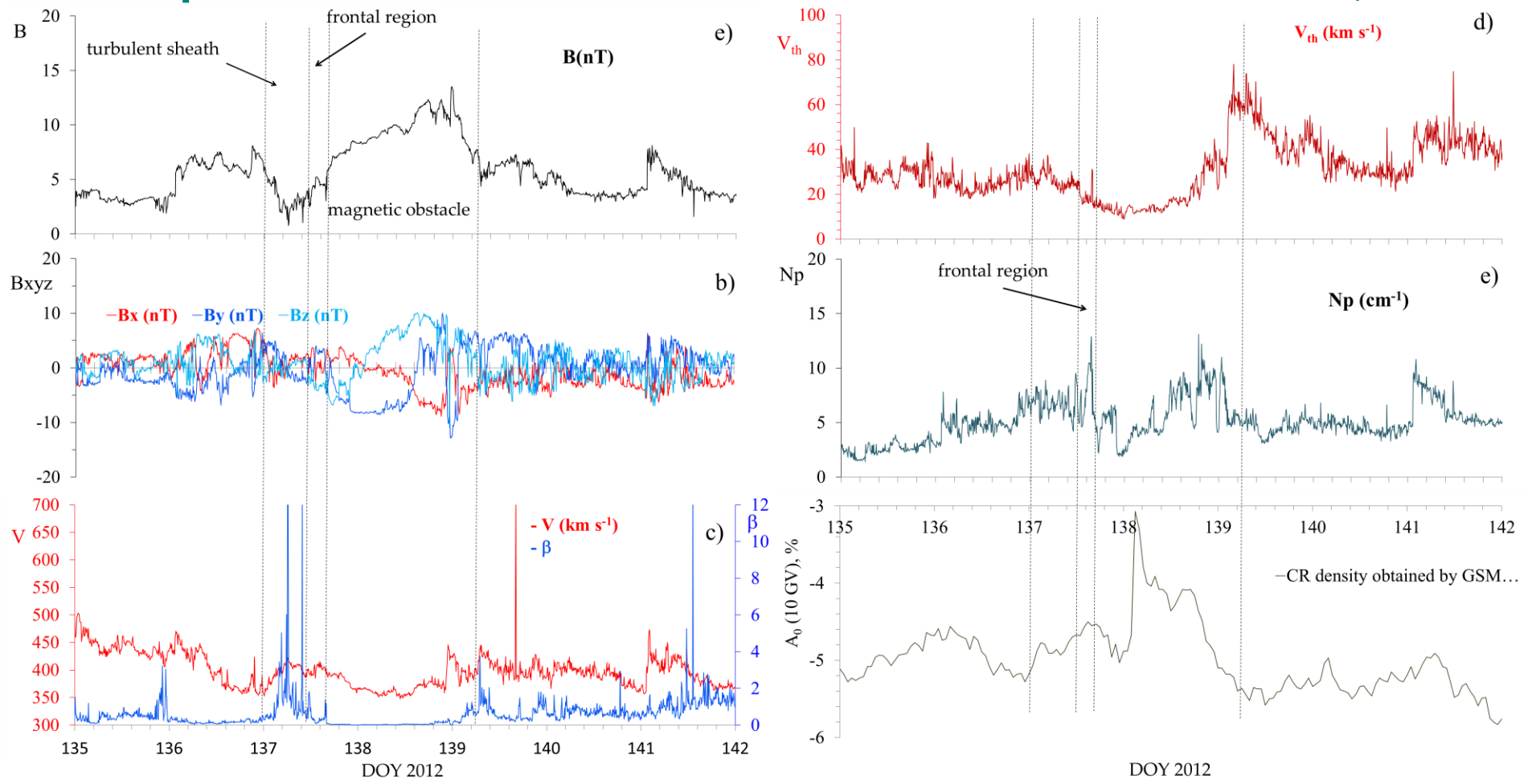

the period (DOY = 194 - 200) from 12 to 18 July 2012

IV) Example of an isolated Earth-impacting where **TS + FR and MO itself caused increase/decrease of CR density**. Belov+ (2015)

One step CR variation profile (7/17, 41%) / Two step profile CR variation (9/17, 53%) / Increase (1/17, 6%)

ICMEs - SW parameters vs CR variation

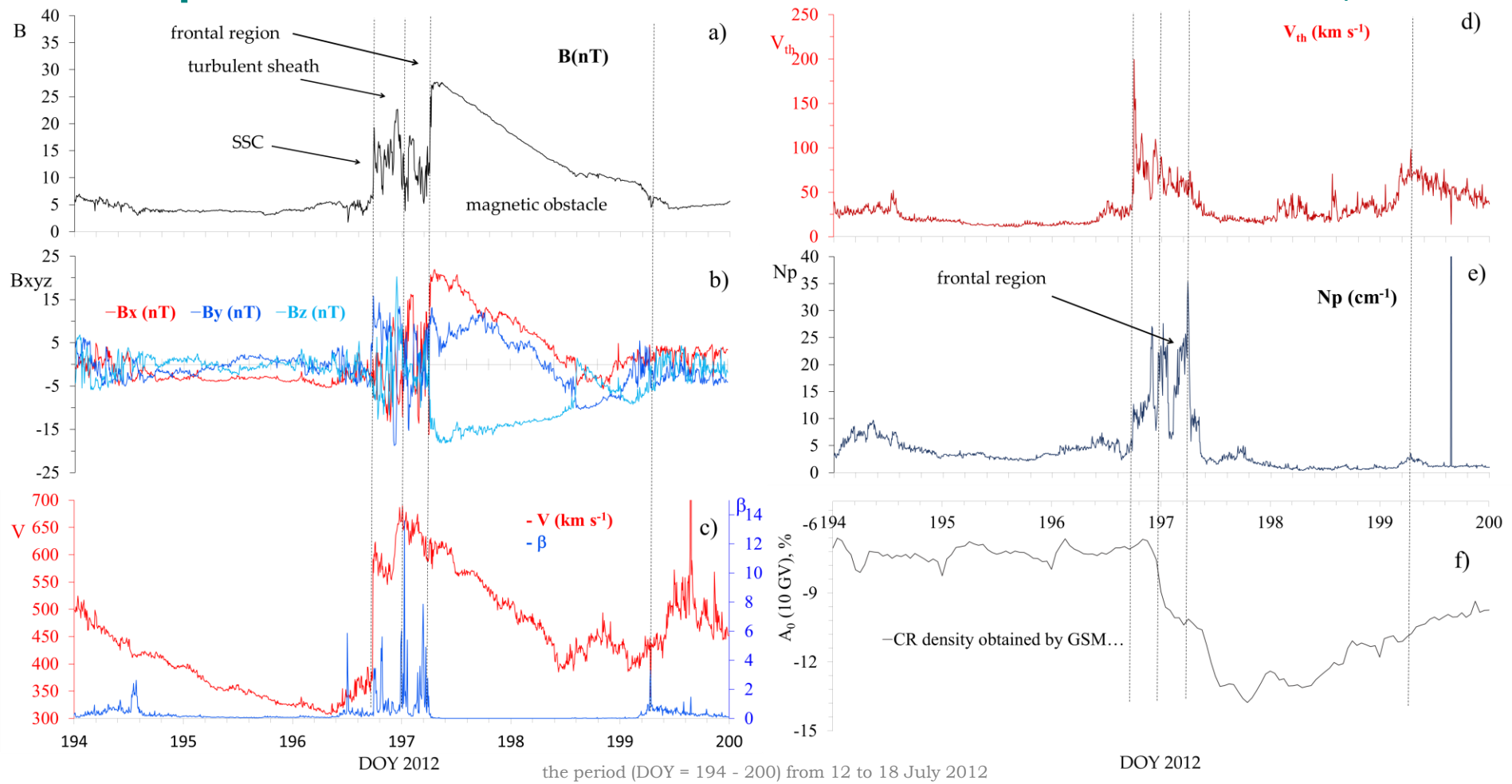

the period (DOY = 194 - 200) from 12 to 18 July 2012

I) Example of an isolated Earth-impacting where **MO and TS + FR caused roughly equal variation of CR density** / (59% roughly equally effective in producing the depression) / **two-step profile**

(a) magnetic field magnitude, (b) GSE magnetic field components, (c) solar wind speed and plasma-betapharameter, (d) thermal velocity, (e) proton density, and (f) the variation of CR density at a fixed rigidity of 10 GV.

ICMEs - SW parameters vs CR variation

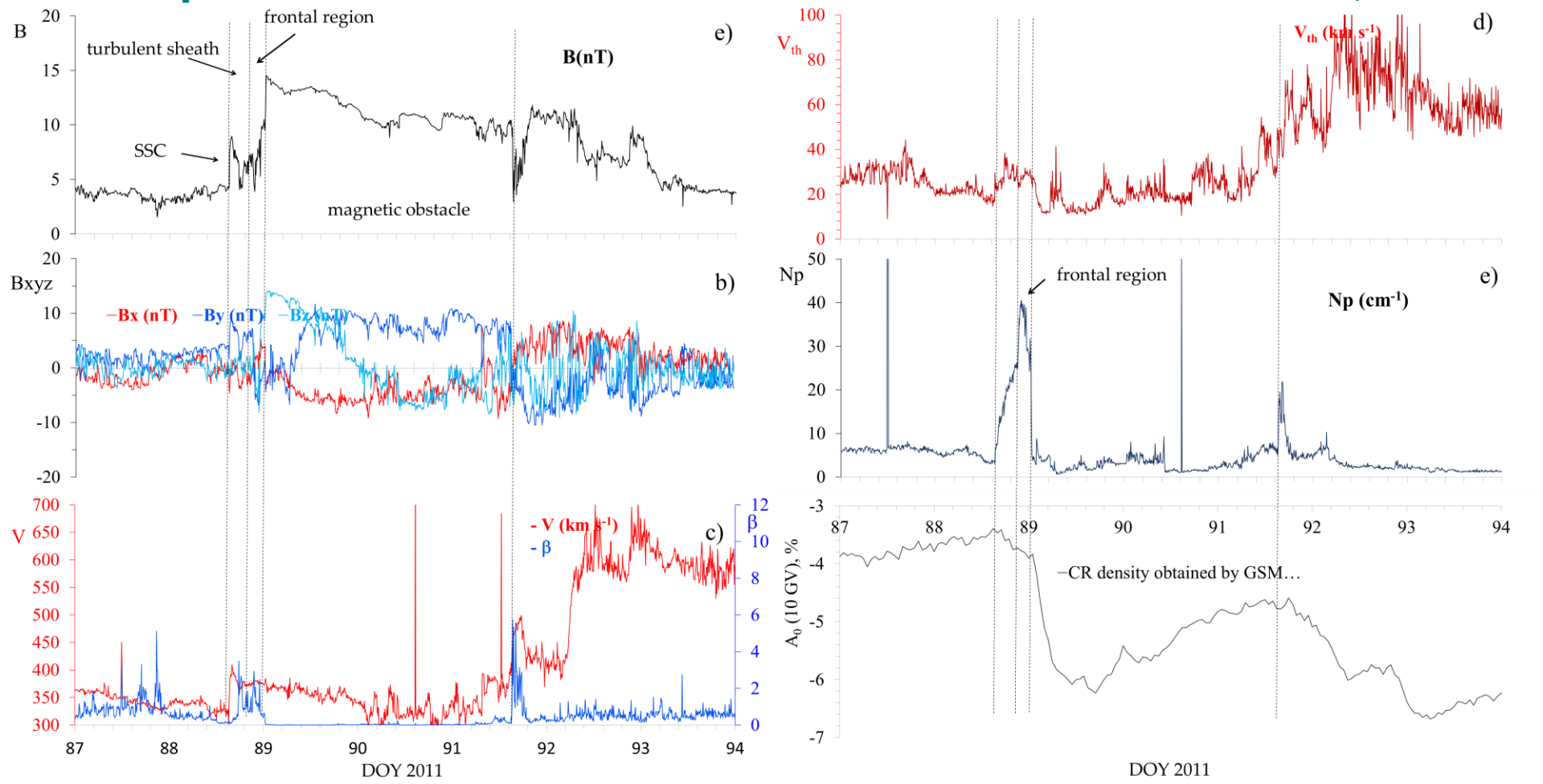

the period (DOY = 87 - 94) from 28 March to 4 April 2011

II) Example of an isolated Earth-impacting where **MO caused significantly stronger variation of CR than TS + FR**. (4/17, 24%)

(a) magnetic field magnitude, (b) GSE magnetic field components, (c) solar wind speed and plasma-beta (plasma-to-magnetic pressure ratio), (d) thermal velocity, (e) proton density, and (f) density of the CR a rigidity of 10 GV.

ICMEs - SW parameters vs CR variation

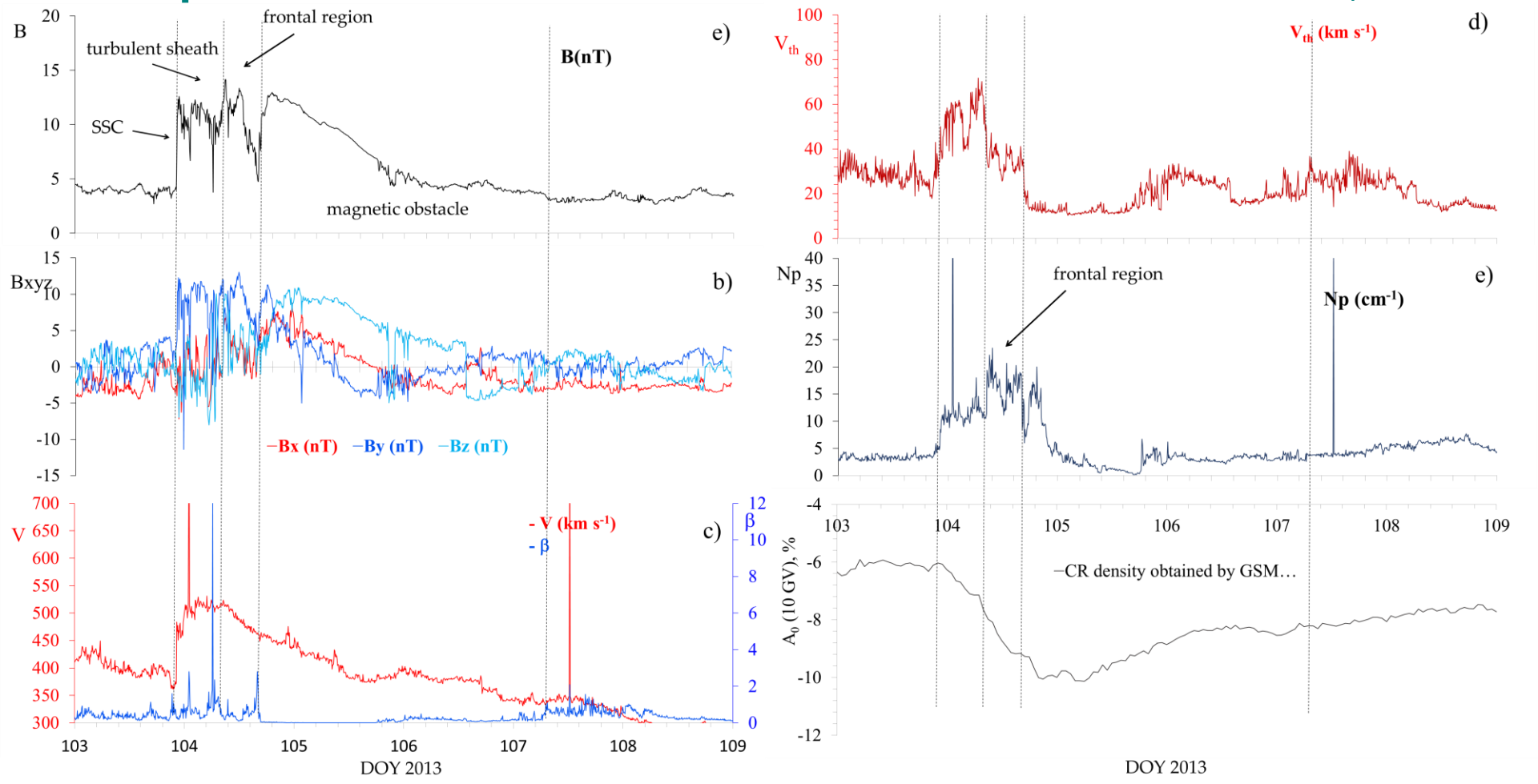

the period (DOY = 194 - 200) from 12 to 18 July 2012

III) Example of an isolated Earth-impacting where **TS + FR caused stronger variation of CR than MO itself**. (2/17, 12%).

(a) magnetic field magnitude, (b) GSE magnetic field components, (c) solar wind speed and plasma-beta (plasma-to-magnetic pressure ratio), (d) thermal velocity, (e) proton density, and (f) density of the CR a rigidity of 10 GV.

Results – SW parameters vs CR variation

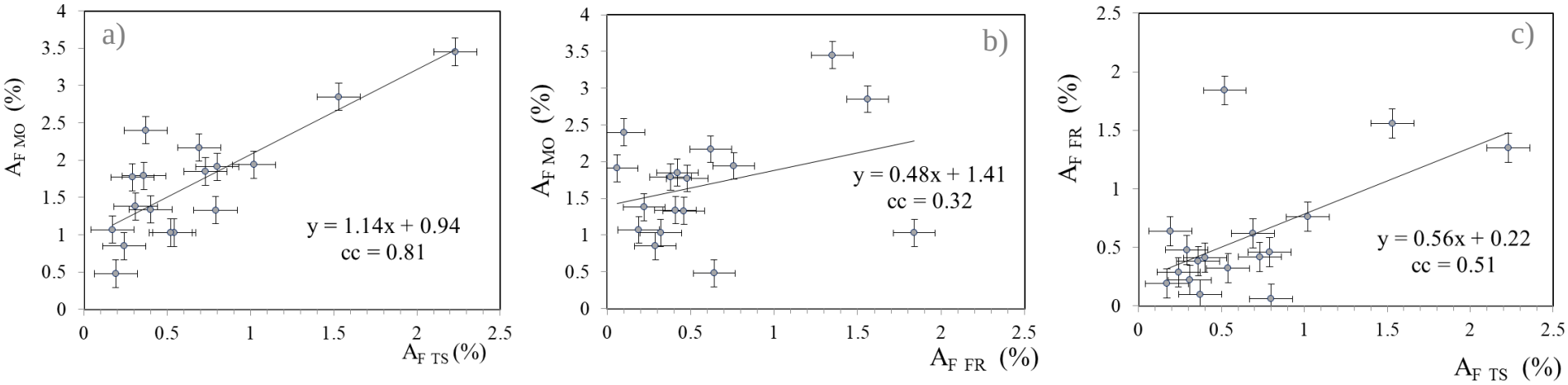

Correlation between the magnitude of variation of CR density, A_F, in the three diffrenet segments of the isolated Earth-directed ICMEs:

panel **a)** turbulent sheat (TS) vs. magnetic obstacle (MO)
panel **b)** frontal region (FR) vs. magnetic obstacle (MO)
and
panel c**)** turbulent sheat (TS) vs. frontal region (FR)

Note that some points overlap.

Results – SW parameters vs CR variation

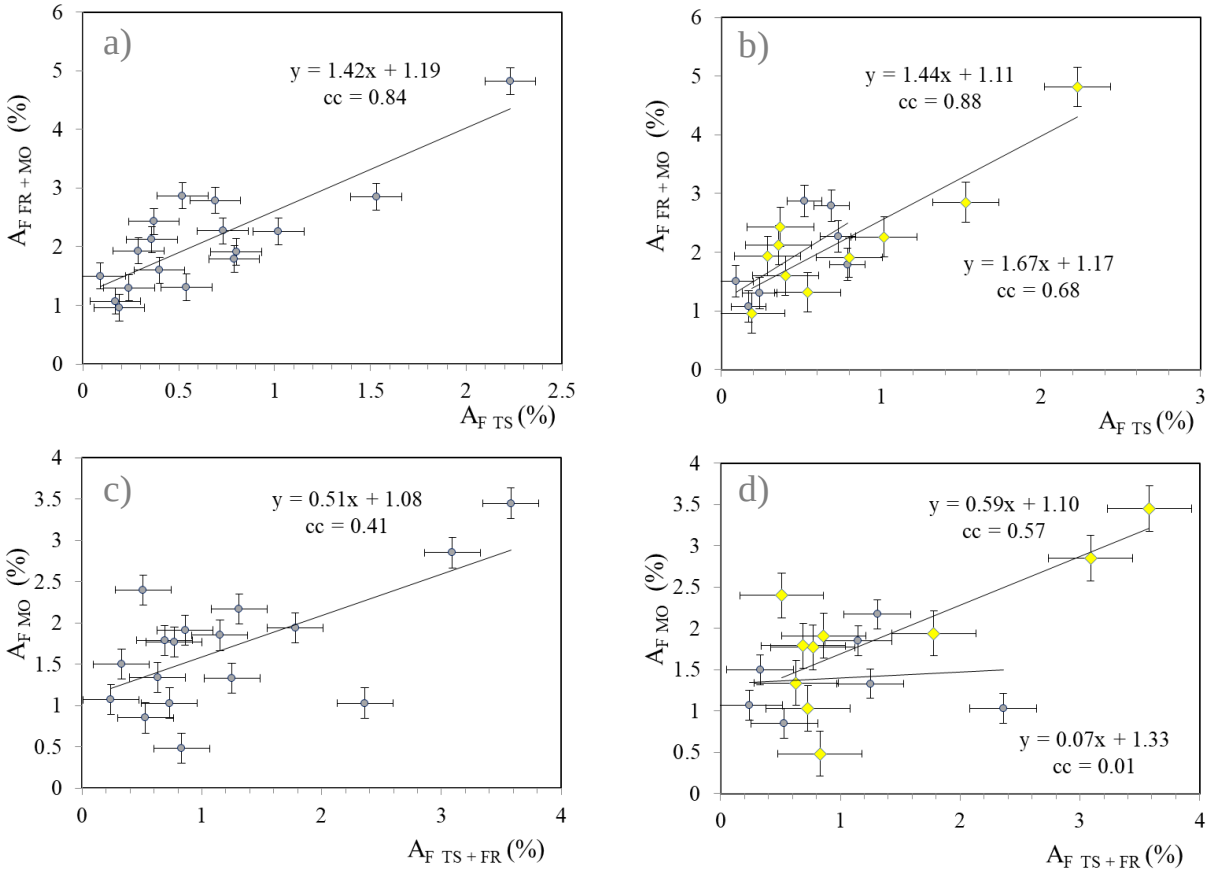

Correlation between the magnitude of variation of CR density, A_F, in the two diffrenet segments of the isolated Earth-directed ICMEs:

panel **a)** turbulent sheat (TS) + frontal region (FR) vs. magnetic obstacle (MO)
and
panel **b)** turbulent sheat (TS) vs. frontal region (FR) + magnetic obstacle (MO)
Note that some points overlap.

Results

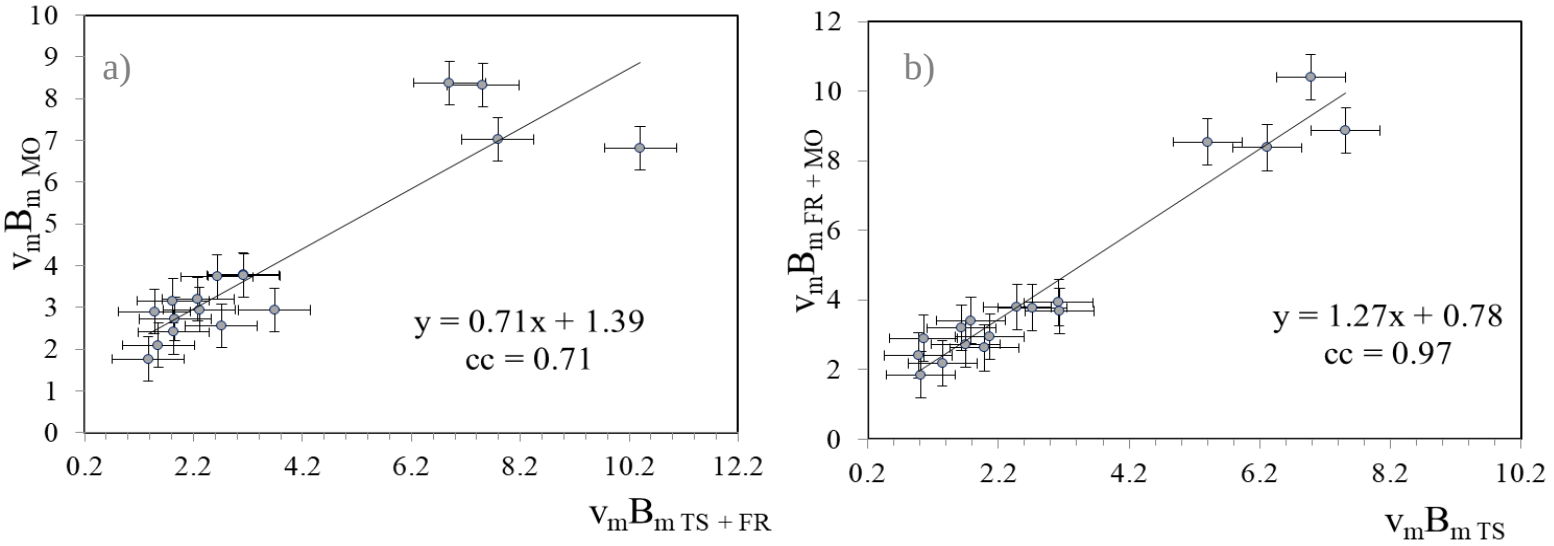

$V_m B_m$ the normalized product of the maximum SW velocity and the IMF intensity, which is the most effective characteristic of the interplanetary disturbance to correlate with different parameters.

where V_0 and B_0 are the typical parameters of the undisturbed interplanetary space.

$$V_m B_m = \frac{V_{\max}}{V_0}\frac{B_{\max}}{B_0}$$

We take V_0 = 400 kms−1, B_0 = 5 nT, B_{max} (in nT) and V_{max} (in kms^{-1}) as the maximum intensity of the IMF and the SW velocity in the disturbance.

Results

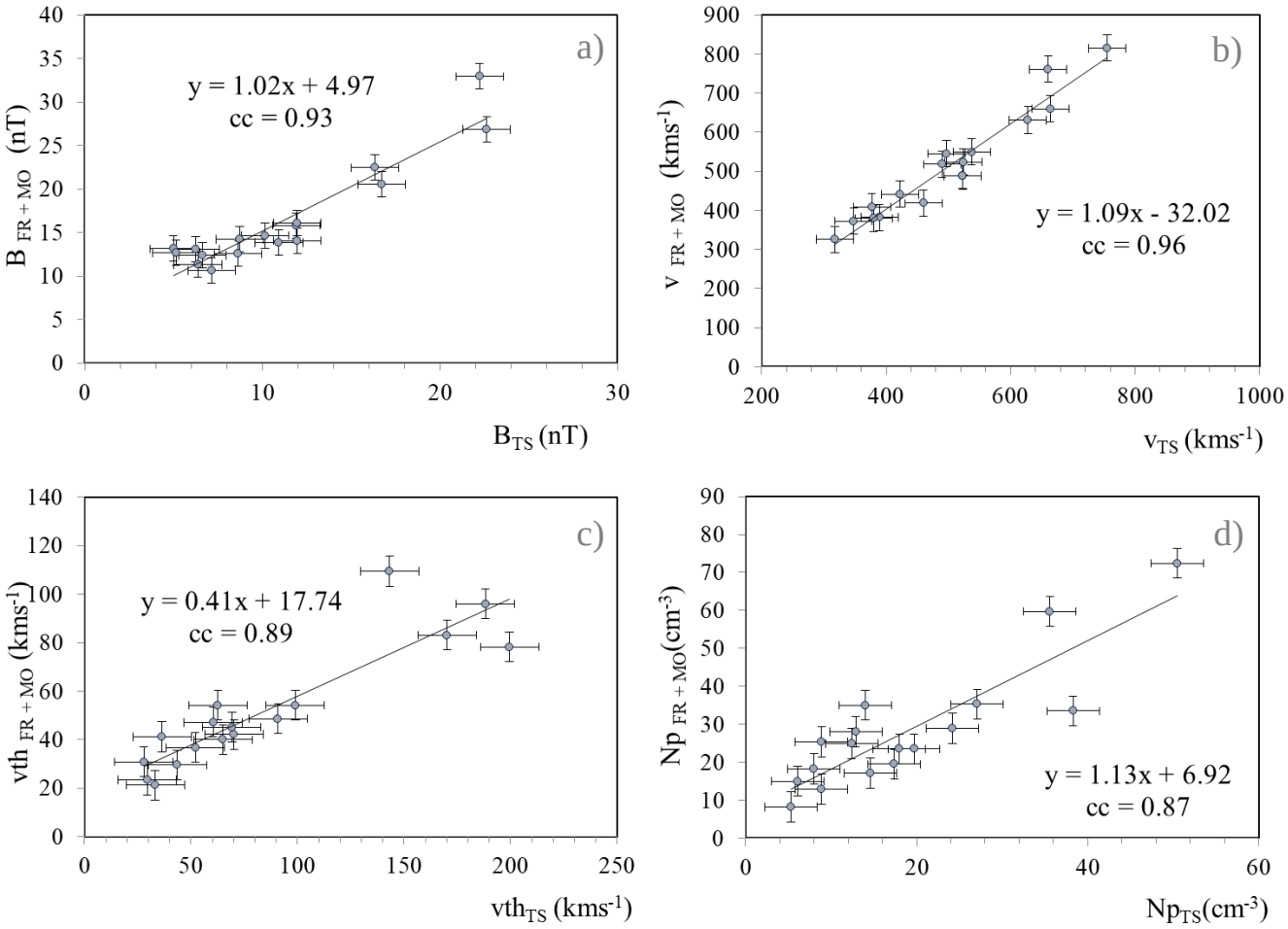

TS vs. FR + MO correlations of: a) the maximum magnetic field magnitude, B_{max}; b) the solar wind speed, v_{max}; c) the proton thermal speed, v_{th}; and f) the proton density, Np.

Results

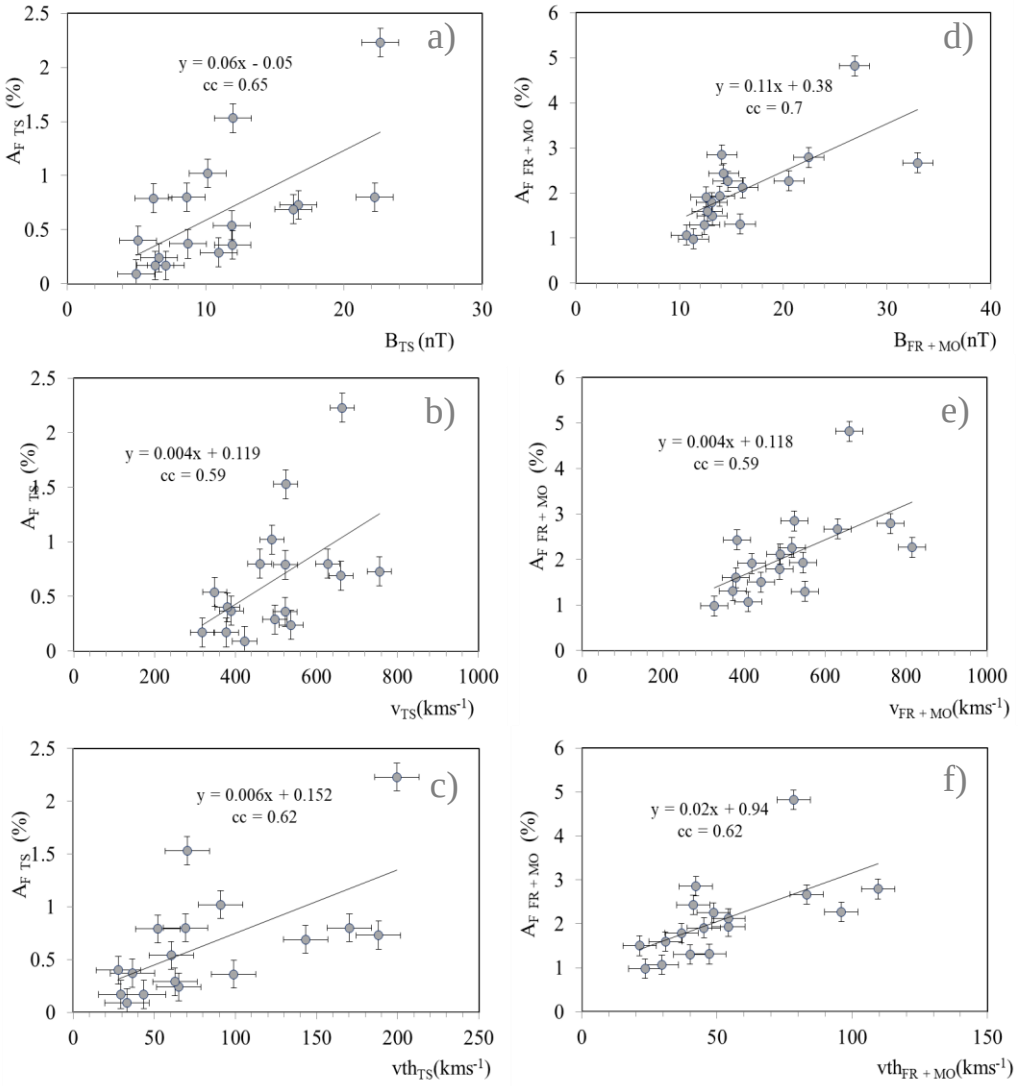

correlations of A_F caused by TS vs. FR + MO structural elements of ICME with: a) the maximum magnetic field magnitude, B_{max}; b) the solar wind speed, v_{max}; and, c) the proton thermal speed, v_{th}.

Results

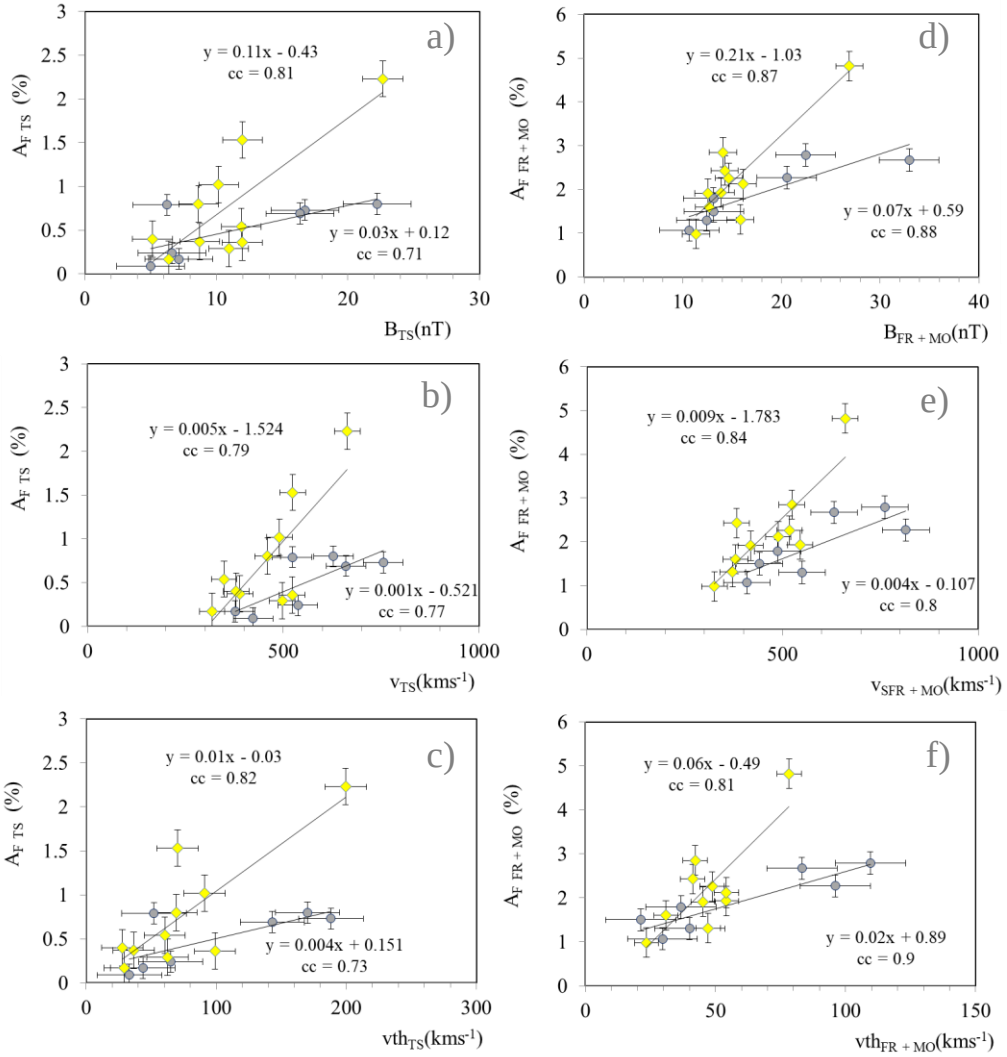

correlations of A_F caused by TS vs. FR + MO structural elements of ICME with: a) the maximum magnetic field magnitude, B_{max}; b) the solar wind speed, v_{max}; and, c) the proton thermal speed, v_{th}.

Conclusions

from the analysis of SW disturbances ⇒ we found 282 solar wind disturbances from 2008 to 2014 (7 years period).

removing ICMEs signatures ⇒ from elogation-time, using HM approximation, we calculated direction and arrival time of ICME at Earth distance. 103 CMEs can be connected with 67 corresponding SW disturbance.

clasification of SW signatures ⇒ for the 7 year period we established 17 isolated Earth directed ICMEs.

from analysis of the SW parameters vs variation of CR density ⇒
A strong correlation is found between four basic solar wind parameters, magnetic field magnitude, B_{max}; proton thermal speed, v_{th}; flow speed, v; and the proton density, Np; between TS and FR+ MO structural elements of ICME, with: cc = 0.93, 0.89, 0.96 and 0.87, respectively. While we did not find such a strong correlation between TS + FR (together) vs. MO segments of ICME.
In the case of magnitude of CR variation, A_F; corelation between by TS + FR vs. MO itself, is cc = 0.42, while we found strong corelation for, A_F; between by TS vs FR + MO, correlations are characterized by higher values, cc = 0.84 .

in future ⇒ (IZMIRAN DATA) use Global Survey Method (GSE) method for aditional analysis, find more events in the new solar cycle.

THANK YOU FOR ATTENTION

Results – data form RC catalogue of ICME

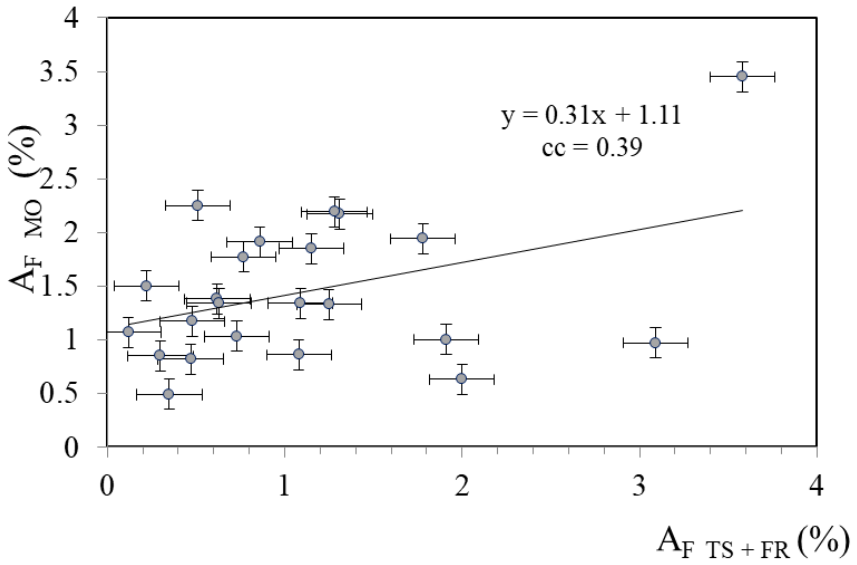

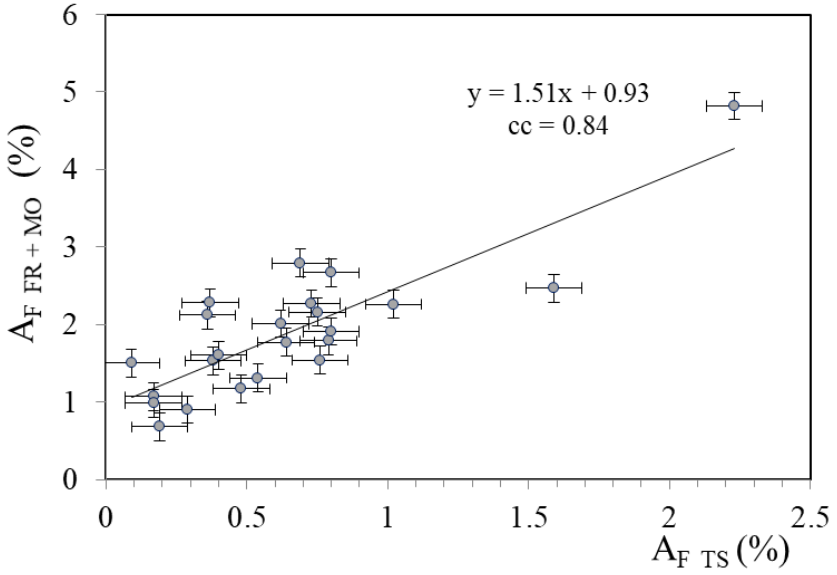

Correlation between the magnitude of variation of CR density, A_F, in the two different segments of the isolated Earth-directed ICMEs:

panel **a)** turbulent sheat (TS) + frontal region (FR) vs. magnetic obstacle (MO)
and
panel **b)** turbulent sheat (TS) vs. frontal region (FR) + magnetic obstacle (MO)
Note that some points overlap.

Direct or flank

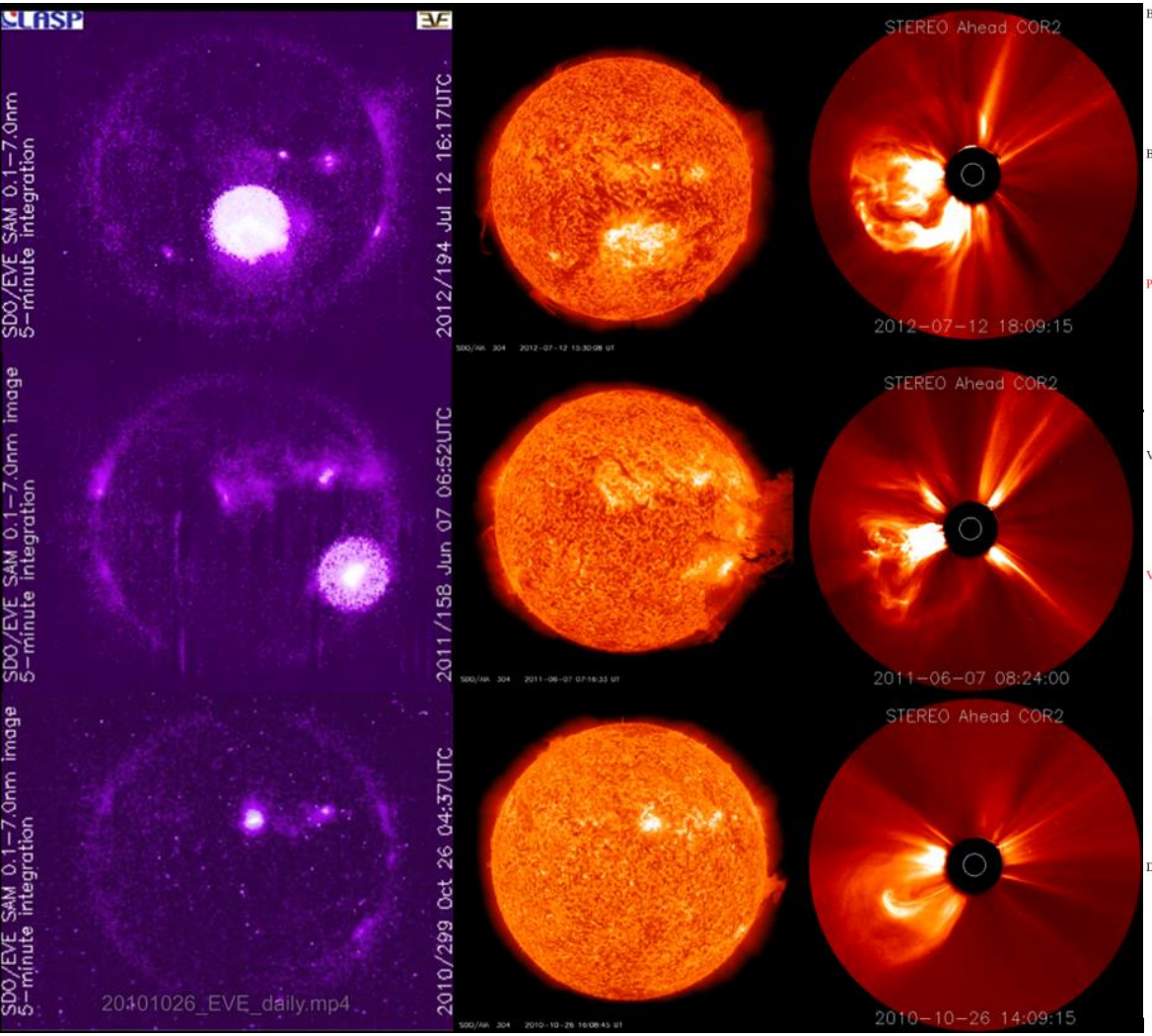

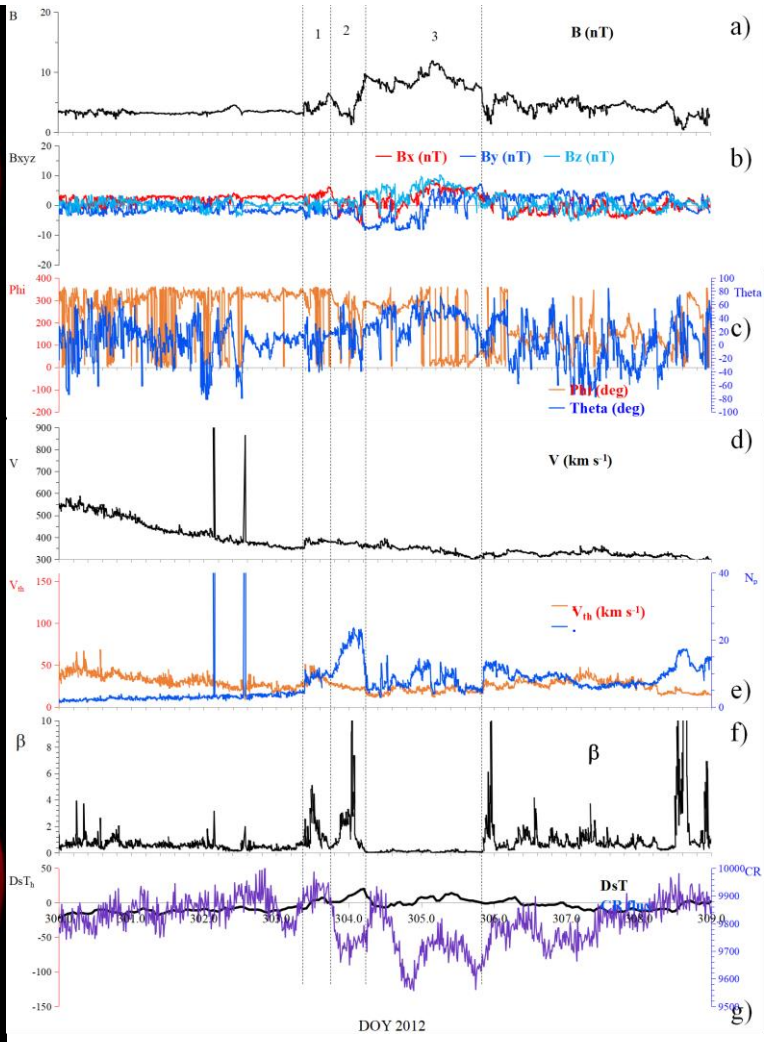

(13% of total ICME and ~2% whole SW, sample)
Stealth ICME; example 26 Oct 2010

the period (DOY = 300 - 309) from 26 October to 4 November 2012

Direct or flank

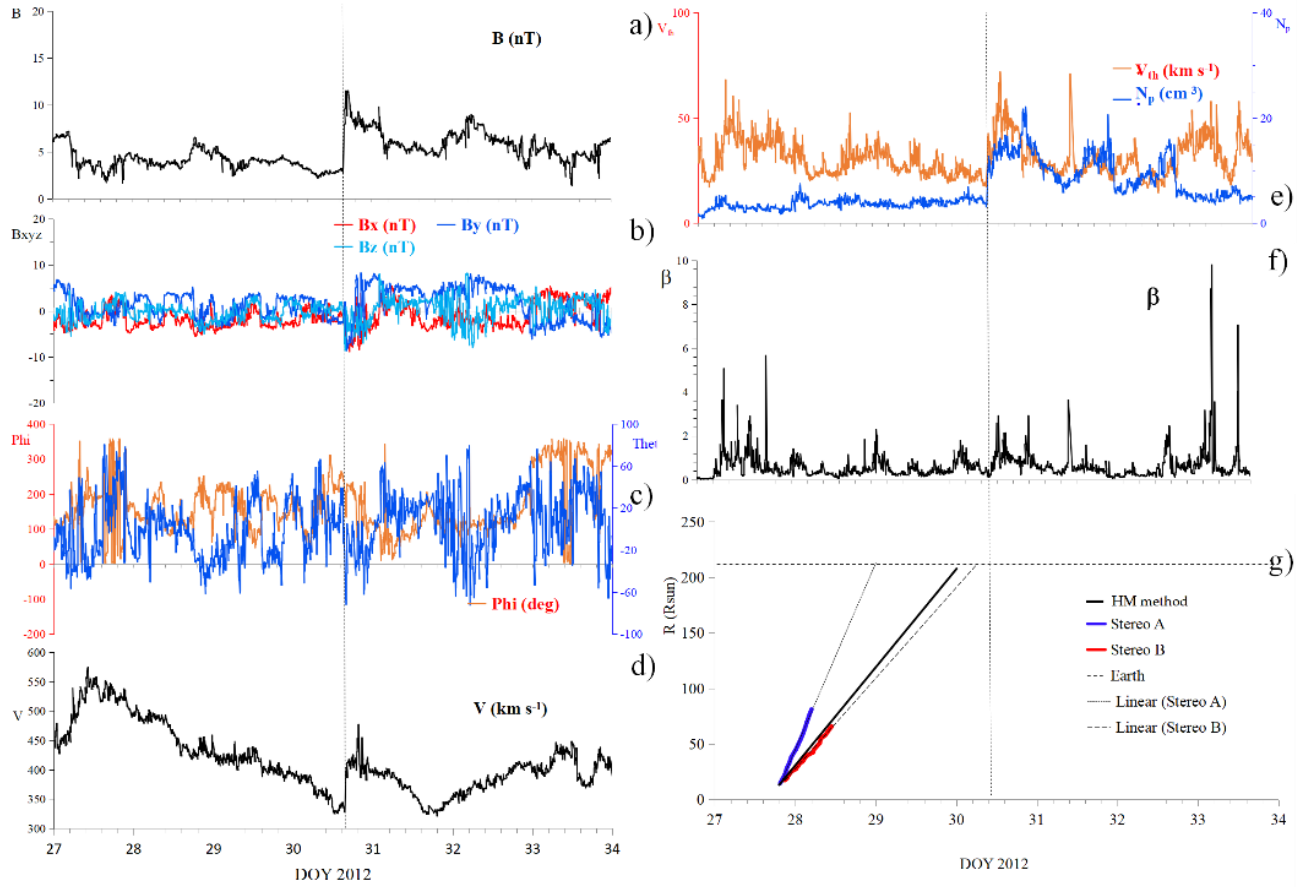

figure form Kim et al. (2013)

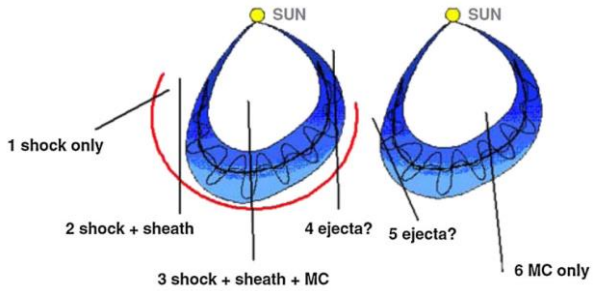

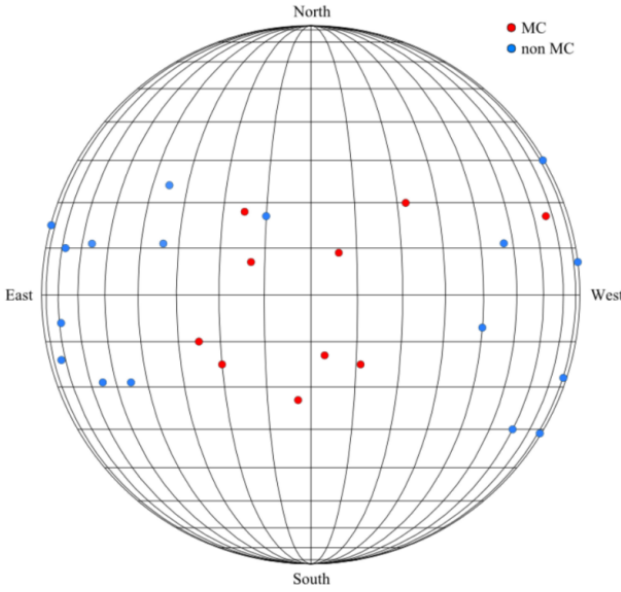

from 39 single ICMEs signatures: 18 direct and 21 flank;

ICMEs – frontal region vs turbulent sheat

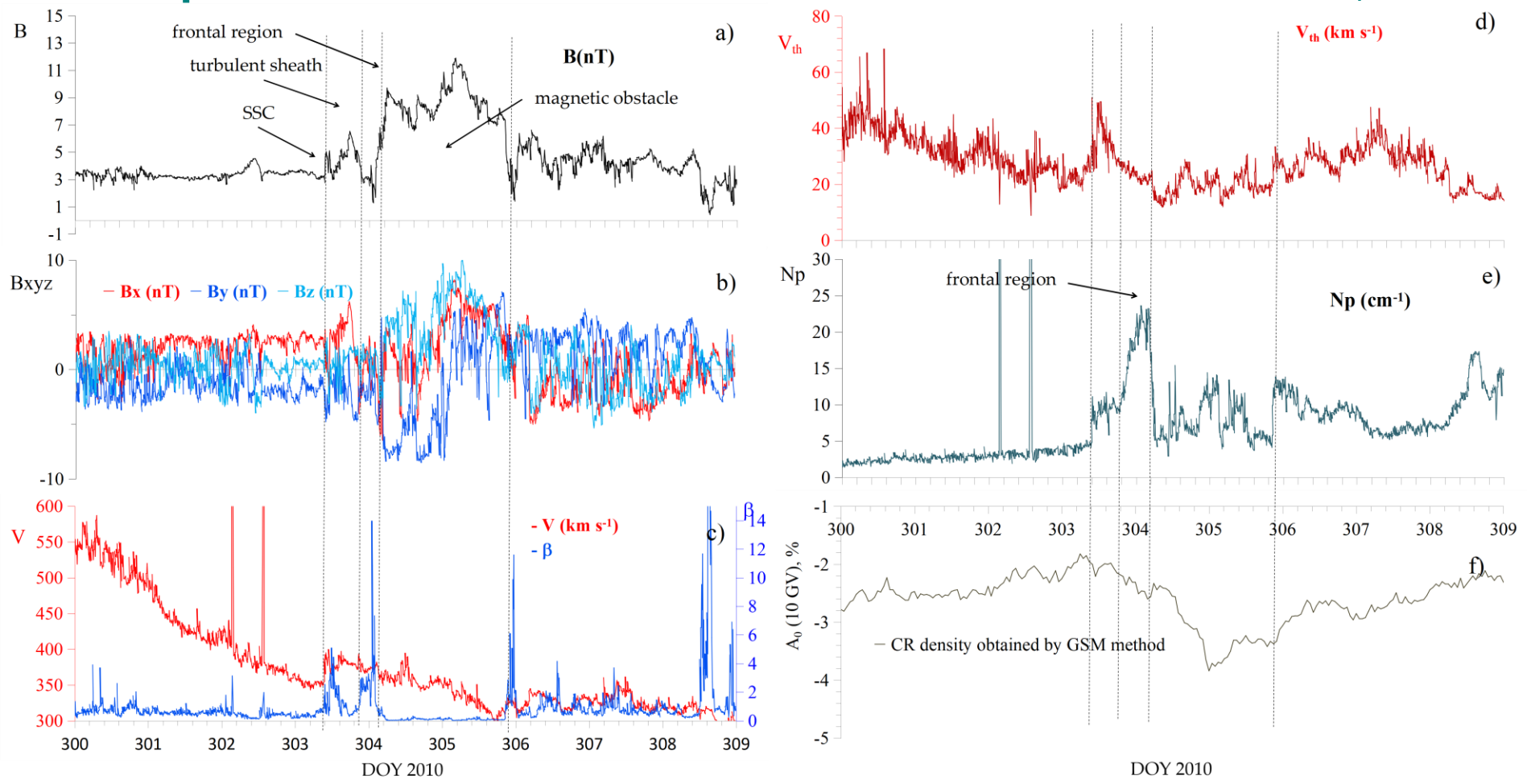

the period (DOY = 300 - 309) from 27 October to 5 November 2010

II) Example of an isolated Earth-impacting where **MO caused much stronger variation of CR than TS + FR**. (4/17, 24%)

(a) magnetic field magnitude, (b) GSE magnetic field components, (c) solar wind speed and plasma-beta (plasma-to-magnetic pressure ratio), (d) thermal velocity, (e) proton density, and (f) density of the CR a rigidity of 10 GV.

MO- or EJ- ICMEs

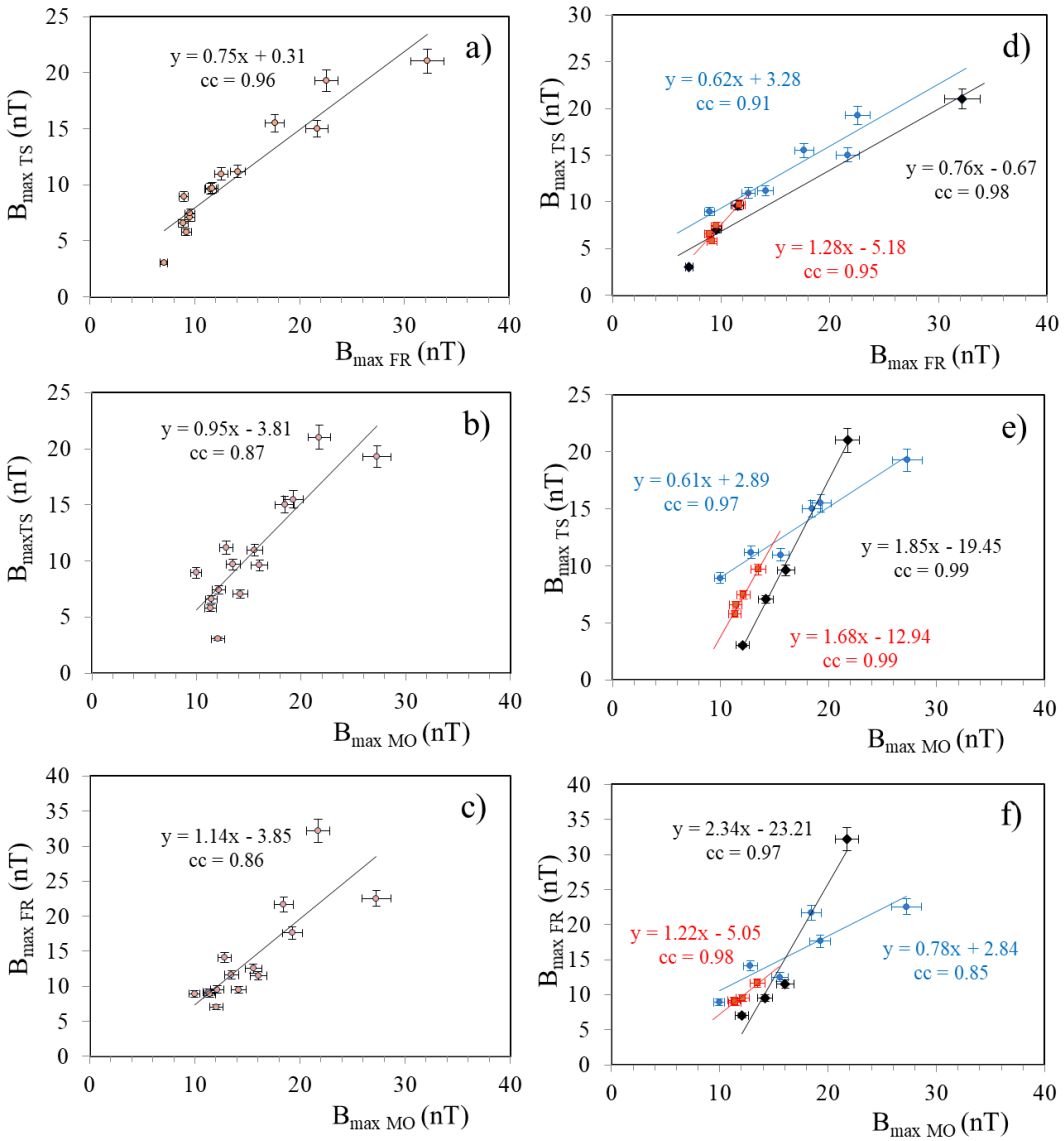

Correlations between the maximum magnetic field magnitude, Bmax, in the three different segments of MO-ICMEs:
turbulent sheath (TS),
frontal region (FR), and
magnetic obstacle (MO).

In panels d, e, and f, plots analogous to those in panels a, b, and c are shown, but the ICMEs are divided into different (filament) types:
AR-events (blue),
DSF-events (black), and
Stealthy CMEs (red).

from Maričić+ (2020)

Distinct correlations are found between the values of Bmax for all filament types.